



# Incorporating multimodal coordination into timetabling optimization of the last trains in an urban railway network

Kang Huang <sup>a,b,c</sup>, Jianjun Wu <sup>a,\*</sup>, Feixiong Liao <sup>b,\*</sup>, Huijun Sun <sup>c</sup>, Fang He <sup>d</sup>, Ziyou Gao <sup>a</sup>

<sup>a</sup> State Key Laboratory of Rail Traffic Control and Safety, Beijing Jiaotong University, Beijing, China

<sup>b</sup> Urban Planning and Transportation Group, Eindhoven University of Technology, Eindhoven, the Netherlands

<sup>c</sup> School of Traffic and Transportation, Beijing Jiaotong University, Beijing, China

<sup>d</sup> Department of Industrial Engineering, Tsinghua University, Beijing, China



## ARTICLE INFO

### Keywords:

Urban rail transit

Last train

Timetabling

Multimodal coordination

## ABSTRACT

Urban rail transit (URT) provides efficient and low-cost services for passengers. It is a common issue for operators to coordinate the last trains of a URT network. This paper discusses three models in a progressive fashion to optimize the last train timetable incorporating multimodal coordination. The first model maximizes the transferability at transfer stations without the distinction of the stations. The second model, based on a refined classification of stations and lines, optimizes the transferability at transfer stations between different transport modes. The third model maximizes the multimodal coordination taking into account the space-time distribution of the arrivals and departures of the connecting modes. These models are formulated as mixed-integer linear programming by linearization techniques for finding the optimal timetable solutions. The proposed models are tested in the Beijing URT network connecting three railway stations and two airport terminals. The numerical results indicate that the proposed models can effectively improve the coordination among the last trains within the URT network and between the URT and the connecting modes.

## 1. Introduction

Urban rail transit (URT) provides secure and punctual passenger mobility services in large volume and plays an increasingly important role in alleviating road congestion and reducing energy consumption. The total length of the URT worldwide has been rising rapidly recently. For instance, in China, 35 cities had URT with a total length over 4750 km in 2017 and the total length will be 6000 km in 2020 (Huang et al., 2019). Passenger mobility and travel demand, especially in mega-cities, rely heavily on URT. For example, the Beijing URT affords 3.85 billion ridership in 2018 with a growth rate of 1.9% annually according to the 2019 Beijing Transport Annual Report.<sup>1</sup>

Much research has been focusing on improving the services of the URT (Wong et al., 2008; Niu and Zhou, 2013; Wu et al., 2015; Niu et al., 2015; Canca and Zarzo, 2017; Guo et al., 2018; Sun et al., 2018; Canca, and Barrena, 2018; Shang et al., 2019; Lv et al., 2019; Zhang et al., 2019; Guo et al., 2020; Yang et al., 2020). Several main research subjects include the network design (Jin et al., 2013; An

\* Corresponding authors.

E-mail addresses: [jjwu1@bjtu.edu.cn](mailto:jjwu1@bjtu.edu.cn) (J. Wu), [f.liao@tue.nl](mailto:f.liao@tue.nl) (F. Liao).

<sup>1</sup> Beijing Transport Annual Report, 2019. <http://www.bjtrc.org.cn>List/index/cid/7.html>

and Lo, 2016; Gutiérrez-Jarpa et al., 2018), line planning (Goossens et al., 2006; Fu et al., 2015) and timetabling (Hassannayebi et al., 2016; Hassannayebi and Zegordi, 2017; Shang et al., 2018; Yang et al., 2019a; Hassannayebi et al., 2019; Yang et al., 2019b), rescheduling (Gao et al., 2016; Binder et al., 2017; Ortega et al., 2018; Zhu and Goverde, 2019), and combinations of the above for the planning and operations (Canca et al., 2017; Yue et al., 2017; Yan and Goverde, 2019; Canca et al., 2019). For a developed URT system, the timetabling optimization becomes the most efficient and cost-saving way to maximize their services (such as minimizing transfer time and maximizing transfer accessibility) or to minimize the generalized costs (Guo et al., 2016).

The URT seldom provides full-day (24-h) services due to the low ridership and the need for maintenance at night. Therefore, there is a special and practical timetabling problem of the last trains in the URT system in the late evening. If the connection at the transfer station fails, the passengers who need transfers in the URT system cannot reach their destinations. Therefore, the last train timetabling problem (LTTP) has drawn much attention (Zhou et al., 2013; Dou et al., 2015; Dou and Guo, 2017; Xu et al., 2018; Zhou et al., 2019).

The LTTP in the past research focused on the coordination at transfer stations (referred to as ST-LTTP by Zhou et al. (2019) for station-transferability based LTTP). Kang et al. (2015a) proposed a model to reveal the relationships between passenger transfer connection time and waiting time with the aim of maximizing the transfer connection headways, and developed a solution algorithm based on genetic algorithm (GA). Kang et al. (2015b) further suggested a method to find a timetable minimizing the deviation from the original timetable and maximizing the average transfer redundant time and the network accessibility. To minimize the standard deviation of transfer redundant times and balance the last train transfers in subway networks, a non-linear optimization model and a heuristic algorithm were developed by Kang and Zhu (2017). To deal with large-scale URT networks, Kang and Meng (2017) put forward a global optimization model in a mixed-integer linear (MIL) formulation. A two-phase decomposition method was proposed to solve the large-scale problems globally by decomposing the original MIL model into two MIL models. Yang et al. (2017) considered the decision-makers' risk preferences under uncertainty and formulated an optimization model for the last train timetabling that explicitly considers the number of successful transfers and the running times of last trains, for which a tabu search algorithm was employed to find the solutions. From the viewpoint of balancing different objectives of the transport operators, a bi-level programming model was proposed by Yin et al. (2019). The upper level aimed to improve the social service efficiency and the lower level to cut down the revenue loss for the operators. Since the URT is not only the transport mode for city trips, Kang et al. (2019) paid attention to the synchronization between URT and other modes (e.g., bus). They presented an optimization-based approach that deposed the LTTP by developing a mixed-integer linear programming (MILP) model to bridge coordination between the last trains and buses. To maintain model tractability, they decomposed the model into two smaller MILP models: maximizing the last train connections and minimizing the waiting times of rail-to-bus passengers.

Recently, some research concerned the origin-destination (OD) accessibility in the URT system (referred to as DR-LTTP by Zhou et al. (2019) for destination-reachability based LTTP). Yao et al. (2019) presented a bi-level model framework to maximize the number of passengers served by the last trains and minimize their transfer waiting time at the upper lever, considering passenger path choice with a detour routing strategy at the lower level. The solution of the upper-level model was found by a GA, and the lower level model was solved by a semi-assignment algorithm. Chen et al. (2019b) suggested three models in a progressive relationship. First, a basic model fine-tuned the last train timetable given the bounds of dwell time. Then, allowing mutual transfers with the prolonged dwell time to maximize transfer accessibility, a bi-objective model was proposed to seek the trade-off between the transfer accessibility and the dwell time extension. Finally, they treated the heterogeneity of transfer walking time as a random variable and employed a discrete approximation of the nonlinear model. To maximize the accessible OD pairs for last train services, a MIP model was proposed with the objective of maximizing the percentage of passengers who successfully reach their destinations (Chen et al., 2019a). Considering passenger assignment in LTTP, Zhou et al. (2019) formally introduced the DR-LTTP in a MILP and solved the problem by an existing optimization solver.

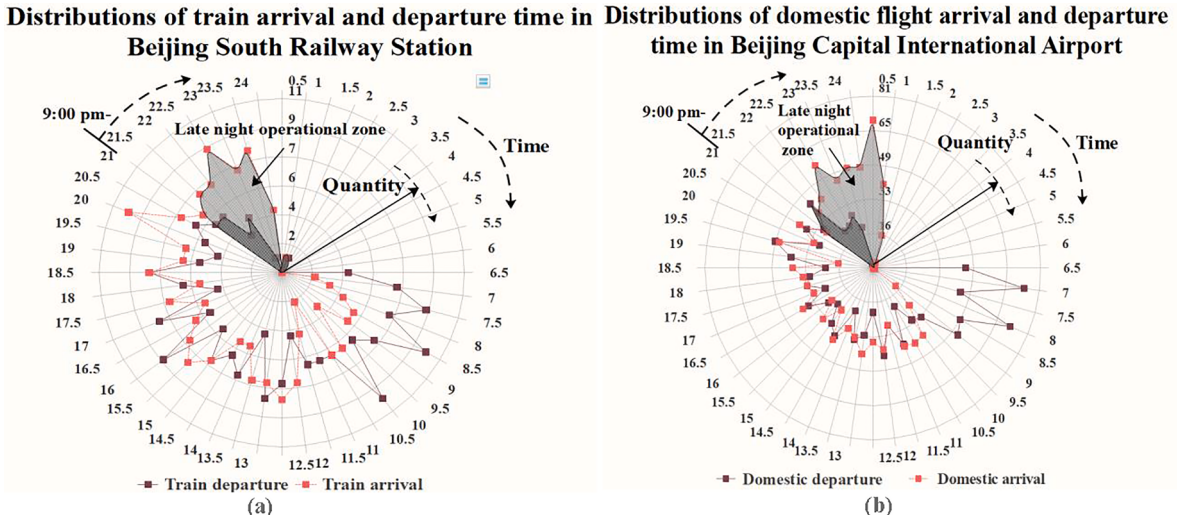


**Fig. 1.** Distributions of the arrival and departure times of railway and airplanes in Beijing.

The above studies have mainly addressed transferability at the stations and destination-reachability for passenger demand. However, several limitations exist in the above problem formulations. First, ST-LTTP focuses on the passengers' transferability only at transfer stations, but the successful transfers at stations do not necessarily imply higher reachability, especially in a large-scale URT network (Zhou et al., 2019). Second, although the DR-LTTP takes into account passengers' path choice in the URT network and is more dedicated to improving individuals' accessibility, it is hard to find the optimal solution in a large-scale network and supposedly difficult than the ST-LTTP due to the vast path permutations. Third, neither of the ST-LTTP and DR-LTTP has incorporated multimodal coordination between URT and other connecting modes. Finally, the space-time distribution of the connecting modes is largely overlooked in the LTTP.

To address the above limitations and pay more attention to the coordination between URT and other modes, we propose a model framework for the LTTP that considers passenger path choice with less complexity and ensures valid transferability and high reachability at transfer stations.

To improve transferability, the space-time distribution of the arrivals and departures of other connecting modes is also incorporated. For instance, as the hubs for railway and airplane, the Beijing railway stations (i.e., Beijing South Railway Station, Beijing West Railway Station, Beijing Railway Station) and the Beijing Capital International Airport involve heavy passenger flows. As exemplified in Fig. 1(a, b), there are quite a few trains and flights arriving and departing in the late evening, which fall within the service time windows of the last trains in the URT system. To present the model framework clearly, three models are discussed in a progressive relationship. First, the basic model maximizes the transferability at transfer stations without station distinction. Then, the second model maximizes the transferability at transfer stations involving other modes. To ensure valid transferability, we classify the stations and lines at different levels and maximize transferability at the key transfer stations. A bi-objective (maximizing transferability at transfer stations without station distinction and maximizing transferability at the key transfer stations) model is transformed into a single objective model by modifying the first objective function as a constraint. The classification of the lines and stations obviate the enumeration of passenger path sets suggested by Zhou et al. (2019), which is almost impossible in large URT networks. Finally, considering the space-time distributions of other connecting modes (i.e., arrival and departure times of different public transit services), the third model maximizes the coordination at the transfer stations for connecting modes, reflecting the valid connections between the last trains of URT to passengers' destination zones. Particularly, the models are different from Chen et al. (2019a) and Zhou et al. (2019) in deposing the passenger path choice process and different from Kang et al. (2019) in guaranteeing valid transferability. The three models are all formulated in a MIL formulation, which can be solved by the existing MIL solvers. Note that the last-second or even the last-third trains are not considered in our models. Despite relevant to the proposed model framework, incorporating these trains would significantly increase the model complexity but achieve limited improvement in the objectives as found in Zhou et al. (2019).

The remainder of the paper is organized as follows. Section 2 formulates the three progressive models considering the coordination between the last trains of the URT and the connecting modes. Section 3 presents a comprehensive case study considering the connection between the URT system and the railway and air transport in Beijing (China). Finally, Section 4 concludes the main contributions and provides suggestions for future research.

## 2. Model

In this section, we introduce the notations and assumptions and present three model formulations progressively. For each model, the objective, constraints, and the relation to the existing studies are discussed.

### 2.1. Notations and assumptions

The following notations are used in the model:

$L$	set of lines in the URT network.
$l$	index of lines.
$S$	set of stations in the URT network.
$s$	index of stations.
$I$	set of modes.
$i$	index of modes.

(continued on next page)

$a_{ls}^m$	arrival time of the last train in direction $m$ of line $l$ at station $s$ .
$d_{ls}^m$	departure time of the last train in direction $m$ of line $l$ from station $s$ .
$r_{ls}^m$	travel time from the starting (first) station to station $s$ in direction $m$ of line $l$ .
$u_{ll's}^{mm'}$	average transfer time from direction $m$ of line $l$ to direction $m'$ of line $l'$ at station $s$ .
$d_l^m$	departure time of the last train in direction $m$ of line $l$ from the starting station.
$z_{ll's}^{mm'}$	0–1 variable: $z_{ll's}^{mm'} = 1$ if passengers can successfully transfer from direction $m$ of line $l$ to direction $m'$ of line $l'$ at stations; otherwise, $z_{ll's}^{mm'} = 0$ .

(continued)

$G(l)$	set of transfer stations on line $l$ .
$H(s)$	set of lines of station $s$ .
$M$	set of directions, $M = \{1, 2\}$ .
$m$	index of direction, $m \in M$ . $m = 1$ and $m = 2$ denote up-direction and down-direction respectively.
$s^k$	index of the $k$ -th layer stations, $k = 1, 2, 3$ .
$l^k$	index of the $k$ -th layer lines, $k = 1, 2, 3$ .
$m^k$	direction of the $k$ -th layer lines, $k = 1, 2, 3$ .
$[t_{lm}^O, t_{lm}^E]$	time range within which the last train in direction $m$ of line $l$ can depart from the starting station.
$e_{ls}^m$	dwell time of the last train in direction $m$ of line $l$ at $s$ .
$U(t)$	indicator for coordination quantity at time $t$ .
$[t_1^O, t_1^E]$	time range for all last trains at the first-layer stations.
$j, J$	index and set for time interval.
$y$	coordination type. $y = 0$ represents the coordination of the arrival of the last train with another mode's departure; $y = 1$ represents the coordination of the departure of the last train with another mode's arrival.
$f_{jl^k s^l m^l}^{y,i}$	pre-calculated time-dependent coordination quantity for mode $i$ at $j$ -th time interval in coordination type $y$ of the last train in direction $m^l$ of line $l^l$ at $s^l$ .
$x_{jl^k s^l m^l}^{y,i}$	0-1 variable, $x_{jl^k s^l m^l}^{y,i} = 1$ when the successful coordination for mode $i$ at $j$ -th time interval in coordination type $y$ of the last train in direction $m^l$ of line $l^l$ at $s^l$ ; otherwise, $x_{jl^k s^l m^l}^{y,i} = 0$ .
$t_{l^k s^l m^l}^{0,i}$	intermediate variable that represents the arrival time ( $a_{l^k s^l}^m$ ) of the last train in direction $m^l$ of line $l^l$ at station $s^l$ .
$t_{l^k s^l m^l}^{1,i}$	intermediate variable that represents departure time ( $d_{l^k s^l}^m$ ) of the last train in direction $m^l$ of line $l^l$ at station $s^l$ .
$w_{ll^k s^l}$	the importance coefficient of station $s^l$ of line $l^l$ in mode $i$ .

### Decision variables

The following assumptions are used to facilitate the development of the model framework.

**Assumption 1.** The capacity of the last trains can meet the passenger demand according to the actual Automatic Fare Collection System (AFC) data. Therefore, the passenger flow is not considered in the current model (Kang and Zhu, 2017).

**Assumption 2.** The passenger transfer times between different lines are fixed as the average, which can effectively reduce the complexity of the timetabling problem (Wong et al., 2008). Also, the walking time is set a little longer than the average transfer time for most passengers (Chen et al., 2019a).

### 2.2. Model 1

Model 1 concerns the connectivity of the last trains at the transfer stations in a URT network. Among the line set  $L$  in the URT network, let  $s$  be a transfer station between lines  $l$  and  $l'$  whose directions are indexed by  $m$  and  $m'$  respectively. Therefore,  $s$  belongs to the intersection of two sets of transfer stations on line  $l$  and line  $l'$ , denoted by  $G(l)$  and  $G(l')$ .  $m \in M$  is a train running direction index, where  $m = 1$  and  $m = 2$  denote the up- and down-direction, respectively. Model 1 addresses a conventional timetabling optimization problem for the coordination of the last trains (one type of ST-LTTP in Zhou et al. 2019). For clarity, we use  $\Omega_1$  to represent the space of all elements in Model 1, where  $\Omega_1 = \{l, l', m, m', s | l, l' \in L, m, m' \in M, s \in G(l) \cap G(l')\}$ . The objective is to maximize the coordination,

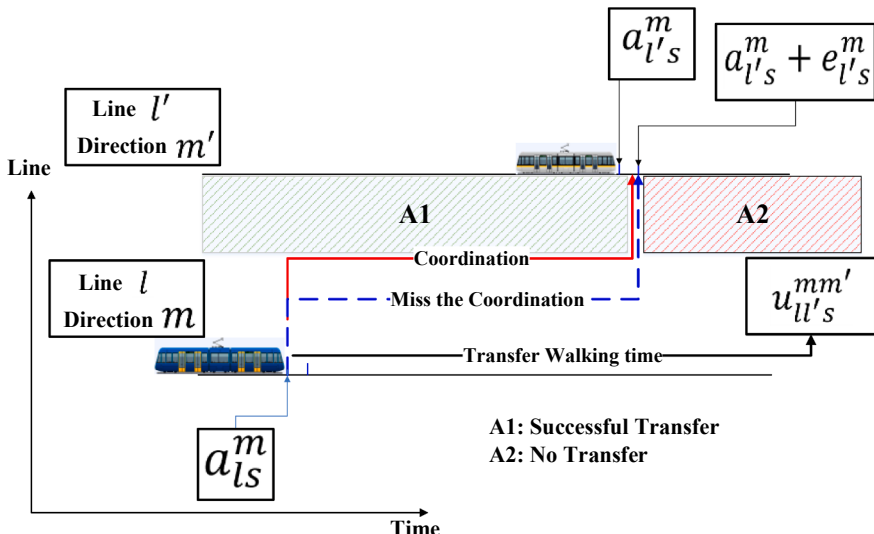


Fig. 2. The space–time requirement for timetabling coordination.

$P_1$ , for all elements in  $\Omega_1$ :

$$\text{Max } P_1 = \sum_{\Omega_1} z_{ll's}^{mm'} \quad l, l', m, m' \in \Omega_1 \quad (1)$$

where  $z_{ll's}^{mm'}$  is a coordination variable:  $z_{ll's}^{mm'} = 1$  if the passengers can successfully transfer from direction  $m$  of line  $l$  to direction  $m'$  of line  $l'$  at stations; otherwise,  $z_{ll's}^{mm'} = 0$ . As illustrated in Fig. 2, for a feeder line  $l$  and a connecting line  $l'$ , when the arrival times of passengers in direction  $m$  of line  $l$  at station  $s$  are earlier than the departure time of the last train in direction  $m'$  of line  $l'$ , the coordination is reached (A1 area,  $z_{ll's}^{mm'} = 1$ ). Otherwise, the passengers cannot make the transfer at  $s$  (A2 area,  $z_{ll's}^{mm'} = 0$ ). Note that the order of line index ( $l$  and  $l'$ ) implies the passengers' transfer direction, but there is no implication of order for  $m$  and  $m'$ . Thus,  $P_1$  is an indicator for the total coordination quantity (CQ) in the URT network to measure the topological connectivity. Similar to the other timetabling problems, Eq. (1) is subject to the following definitional constraints.

#### Departure time constraints:

The departure time from the starting station of the last train in direction  $m$  of line  $l$ ,  $d_l^m$ , should be in the permissible time range  $[t_{lm}^O, t_{lm}^E]$ :

$$t_{lm}^O \leq d_l^m \leq t_{lm}^E, \quad \forall l \in L, m \in M \quad (2)$$

#### Space-time constraints of timetabling coordination:

The arrival time of the last train in direction  $m$  of line  $l$  at station  $s$ ,  $a_{ls}^m$ , is equal to departure time  $d_l^m$  plus travel time  $r_{ls}^m$  as formulated in Eq. (3). Note that  $r_{ls}^m$  is not a decision variable.

$$a_{ls}^m = d_l^m + r_{ls}^m \quad (3)$$

The condition for the coordination is formulated as

$$z_{ll's}^{mm'} = \begin{cases} 1, & \text{if } a_{ls}^m + u_{ll's}^{mm'} \leq a_{ls}^m + e_{ls}^m \\ 0, & \text{otherwise} \end{cases} \quad (4)$$

where  $u_{ll's}^{mm'}$  is the average transfer time from direction  $m$  of line  $l$  to direction  $m'$  of line  $l'$  at station  $s$ , while  $a_{ls}^m$  and  $e_{ls}^m$  are the arrival time and dwell time of the last train in direction  $m$  of line  $l$  at  $s$ . Note that,  $u_{ll's}^{mm'}$  and  $e_{ls}^m$  can be given as input.

Eq. (4) can be linearized by introducing a large number  $\psi_1$  as

$$a_{ls}^m + u_{ll's}^{mm'} - (a_{ls}^m + e_{ls}^m) \leq \psi_1 \cdot (1 - z_{ll's}^{mm'}) \quad l, l', m, m', s \in \Omega_1 \quad (5)$$

Succinctly, Model 1 can be reformulated as

$$\text{Max } P_1 = \sum_{\Omega_1} z_{ll's}^{mm'}$$

$$\text{st.1} \left\{ \begin{array}{l} t_{lm}^O \leq d_l^m \leq t_{lm}^E \\ a_{ls}^m = d_l^m + r_{ls}^m \\ a_{ls}^m + u_{ll's}^{mm'} - (a_{ls}^m + e_{ls}^m) \leq \psi_1 \cdot (1 - z_{ll's}^{mm'}) \\ l, l', m, m', s \in \Omega_1 \end{array} \right.$$

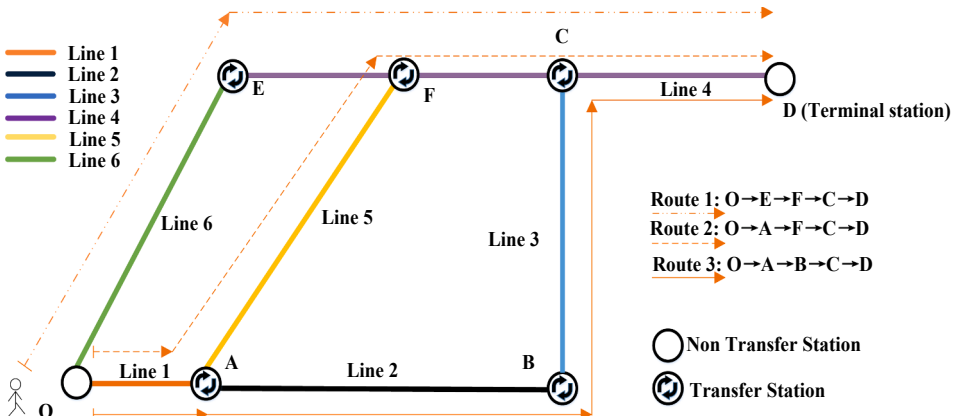


**Fig. 3.** Example of a small URT network with the multimodal connection at station D.

Model 1 is intuitive and simple in formulation for the topological connectivity. However, travel routes and explicit connections with other transport modes have not been considered in Model 1.

### 2.3. Model 2

In Model 2, a new objective function is added to emphasize the coordination of connecting different modes based on a classification of the importance of stations and lines. We first show that ignoring travel routes may cause invalid connections. Taking a simple URT network in Fig. 3 for instance, suppose a passenger needs to reach station D from station O. There are three alternative routes with different transfer times. It is found that no matter which route is chosen, the transfer at Line 4 has to be executed. Route 3 includes three times of transfer, which is commonly considered the worst situation and avoided in a real-world URT network. For Routes 1 and 2, if the connections with Lines 6 and 5 at stations E and F respectively fail by the last trains, the passenger cannot complete the trip even if the connection at station A succeeds. In view of the fact that ordinary transit trips in well-developed URT networks usually involve no more than two transfers, we define the lines in three layers. For example, considering the connection with station D (e.g., a key terminal station for connection modes, airport terminal) of the highest importance, Line 4 is in the first layer directly connecting station D. Lines 5 and 6 are in the second-layer, which need one transfer to reach D. Line 1 is in the third-layer, which needs at least two times of transfer. Similarly, there are three-layer transfer stations. The first-layer station includes D, and the second-layer stations include C, E and F, which are the transfer stations on the first-layer line. The third-layer stations consist of the transfer stations (e.g., A) of the second-layer lines. Therefore, to guarantee coordination among multiple modes, the URT should firstly have successful connections at the second-layer stations (e.g., C, E, and F), and then consider the transferability at the third-layer stations. If the connections at the second-layer stations fail, the passengers cannot reach their destination (e.g., D) and the transferability at third-layer stations (e.g., A) will be omitted. This aspect is integrated in Model 2 and has the advantage of cutting down the complexity when considering all transfer stations for an OD pair simultaneously.

Formally, suppose that the URT connects a set of different modes and the set of the first-layer stations in mode  $i$  is  $R(i)$ ,  $i \in I$ . We introduce a weight coefficient  $w_i$  for the second-layer stations to represent the importance of mode  $i$ . Let  $s^1, s^2$  and  $s^3$  denote a station index of the first, second, and third layer stations respectively.  $l^1, l^2$  and  $l^3$  denote line indices of the first, second, and third layer lines with directions indexed by  $m^1, m^2$  and  $m^3$ , respectively.  $H(s^k)$  ( $k = 1, 2, 3$ ) is the corresponding set of lines including station  $s^k$ .  $G(l^k)$  ( $k = 1, 2, 3$ ) is the set of transfer stations on line  $l^k$ . Thus, we have

$$s^1 \in \bigcup_i R(i), l^1 \in H(s^1), s^2 \in G(l^1), l^2 \in H(s^2), s^3 \in G(l^2) \quad (6)$$

For the second-layer stations, we use  $z_{l^2 l^1 s^2}^{m^1 m^2}$  to represent whether the passengers from the direction  $m^2$  of line  $l^2$  can transfer to the direction  $m^1$  of line  $l^1$  at stations  $s^2$  to access to connecting mode, while  $z_{l^1 l^2 s^2}^{m^1 m^2}$  indicates whether the passengers from the direction  $m^1$  of line  $l^1$  can transfer to the direction  $m^2$  of line  $l^2$  at stations  $s^2$  to egress the connecting mode. When  $z_{l^2 l^1 s^2}^{m^1 m^2} = 1$  and  $z_{l^1 l^2 s^2}^{m^1 m^2} = 1$ , travel route for mode  $i$  is valid. To maximize the valid coordination of the route for the mode, the following objective,  $P_2$ , is formulated.

$$\text{Max } P_2 = \sum_{\Omega_2} w_i \cdot \left( \left( \sum_{\Omega_3} z_{l^2 l^1 s^3}^{m^3 m^2} \right) \cdot z_{l^2 l^1 s^2}^{m^1 m^2} \right) + \sum_{\Omega_2} w_i \cdot \left( \left( \sum_{\Omega_3} z_{l^1 l^2 s^3}^{m^3 m^2} \right) \cdot z_{l^1 l^2 s^2}^{m^1 m^2} \right) \quad (7)$$

$$\Omega_2 = \{i, s^1, l^1, l^2, s^2, m^1, m^2 | \text{Eq.(6)}, m^1, m^2 \in M\};$$

$$\Omega_3 = \{s^3, l^3, m^3 | s^3 \in G(l^3) \cap G(l^2), l^3 \in L, m^3 \in M\}$$

where  $\Omega_2$  is the set of possible transfer at the second-layer stations, and  $\Omega_3$  is the set of possible transfer at the third-layer stations.

The objective function is nonlinear with multiplications of 0–1 variables and integer variables. To linearize the objective function, we introduce a new variable  $\theta$ .

When  $z_{l^2 l^1 s^2}^{m^1 m^2} = 0$ , we have  $\theta_{l^2 l^1 s^2}^{m^1 m^2} = 0$ . When  $z_{l^2 l^1 s^2}^{m^1 m^2} = 1$ ,

$$\theta_{l^2 l^1 s^2}^{m^1 m^2} = w_i \sum_{s^3, l^3, m^3} z_{l^2 l^1 s^3}^{m^3 m^2} \quad s^3, l^3, m^3 \in \Omega_3 \quad (8)$$

Similarly, when  $z_{l^1 l^2 s^2}^{m^1 m^2} = 0$ , we have  $\theta_{l^1 l^2 s^2}^{m^1 m^2} = 0$ . When  $z_{l^1 l^2 s^2}^{m^1 m^2} = 1$ ,

$$\theta_{l^1 l^2 s^2}^{m^1 m^2} = w_i \sum_{s^3, l^3, m^3} z_{l^1 l^2 s^3}^{m^3 m^2} \quad s^3, l^3, m^3 \in \Omega_3 \quad (9)$$

A set of linear constraints can be presented to characterize their relationship as

$$\begin{cases} \theta_{\ell^1 l^2 s^2}^{m^1 m^2} \leq w_i \sum_{s^3, l^3, m^3} z_{l^3 \ell^1 s^3}^{m^3 m^2} + \psi_2 \cdot (1 - z_{\ell^1 l^2 s^2}^{m^1 m^2}) \\ \theta_{\ell^1 l^2 s^2}^{m^1 m^2} \geq w_i \sum_{s^3, l^3, m^3} z_{l^3 \ell^1 s^3}^{m^3 m^2} - \psi_2 \cdot (1 - z_{\ell^1 l^2 s^2}^{m^1 m^2}) \\ \theta_{\ell^1 l^2 s^2}^{m^1 m^2} \leq \psi_2 \cdot z_{\ell^1 l^2 s^2}^{m^1 m^2} \\ \theta_{\ell^1 l^2 s^2}^{m^1 m^2} \geq 0 \end{cases} \quad (10)$$

$$\begin{cases} \theta_{l^1 \ell^2 s^2}^{m^1 m^2} \leq w_i \sum_{s^3, l^3, m^3} z_{l^3 l^1 \ell^3 s^3}^{m^3 m^2} + \psi_2 \cdot (1 - z_{l^1 \ell^2 s^2}^{m^1 m^2}) \\ \theta_{l^1 \ell^2 s^2}^{m^1 m^2} \geq w_i \sum_{s^3, l^3, m^3} z_{l^3 l^1 \ell^3 s^3}^{m^3 m^2} - \psi_2 \cdot (1 - z_{l^1 \ell^2 s^2}^{m^1 m^2}) \\ \theta_{l^1 \ell^2 s^2}^{m^1 m^2} \leq \psi_2 \cdot z_{l^1 \ell^2 s^2}^{m^1 m^2} \\ \theta_{l^1 \ell^2 s^2}^{m^1 m^2} \geq 0 \end{cases} \quad (11)$$

where  $\psi_2$  is a large number. Then,  $P_2$  can be reformulated as

$$\text{Max } P_2 = \sum_{\Omega_2} (\theta_{\ell^1 l^2 s^2}^{m^1 m^2} + \theta_{l^1 \ell^2 s^2}^{m^1 m^2}) \quad (12)$$

Therefore, Model 2 can be formulated as

$$\begin{cases} \text{Max } P_1 = \sum_{\Omega_1} z_{ll^s}^{mm^s} \\ \text{Max } P_2 = \sum_{\Omega_2} (\theta_{\ell^1 l^2 s^2}^{m^1 m^2} + \theta_{l^1 \ell^2 s^2}^{m^1 m^2}) \end{cases}$$

$$st.2 \begin{cases} \text{Eqs.(2) - (5)} \\ \text{Eqs.(10) - (11)} \end{cases}$$

Model 2 is a bi-objective MILP formulation.  $P_1$  represents the topological coordination of the URT network and  $P_2$  attaches importance to the connecting modes. Using a parameter  $\alpha$  to denote a proportion of maximum coordination,  $P_1$  is converted to a constraint as

$$\sum_{m, m^s, l, l^s, s} z_{ll^s}^{mm^s} \geq \alpha P_1^{\max} \quad l, l^s, m, m^s, s \in \Omega_1 \quad (13)$$

Therefore, Model 2 is transformed into a single objective MIL formulation as

$$\text{Max } P_2 = \sum_{\Omega_2} (\theta_{\ell^1 l^2 s^2}^{m^1 m^2} + \theta_{l^1 \ell^2 s^2}^{m^1 m^2})$$

$$st.3 \begin{cases} \text{Eqs.(2) - (5), (10) - (11)} \\ \sum_{\Omega_1} z_{ll^s}^{mm^s} \geq \alpha P_1^{\max} \end{cases}$$

The model can be extended into even more layers with more complicated formulations, for which Eqs. (6)–(12) should be generalized. We have defined the lines in three layers in view of the fact that in real-world applications, ordinary public transit trips in well-developed URT networks usually involve no more than two transfers between three layers of lines.

Model 2 inherits the simple structure of Model 1 and deposes the passenger path choice by ranking the stations and lines and guaranteeing valid transferability with other connecting modes. The classification for the line and station is not complicated and can be listed when considering the several connecting modes. The essence of classification for the line and station resembles the pre-determining set of candidate paths. But it is simpler in the formation and solving process, and less intermediate variable for the set of candidate paths. Even in large networks, listing the classification for the line and station will not be harder than the predetermined set of all candidate paths. To make the optimization model more effective, Model 3 further considers the space-time distribution of the arrivals and departures of the connecting modes in the following.

#### 2.4. Model 3

To consider the connections between different modes in the first-layer stations, we integrate a new objective ( $P_3$ ) and a set of constraints for multimodal trips. We formulate a dynamic coordination function  $U(t)$ , determined at the arrival/departure time  $t$  of the

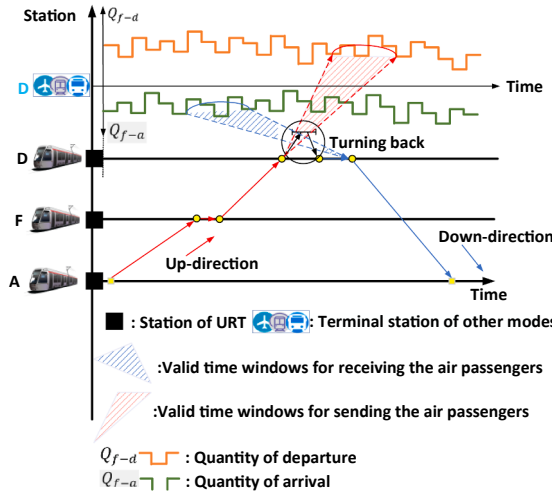


Fig. 4. Last train diagram of connection between URT and airplane mode.

last URT trains. The arrival and departure times are used for justifying whether the passengers can access and egress the connecting modes respectively. Taking Route 2 to the airport (station D) in Fig. 3 for example, an ordinary airplane passenger may conduct a series of preparatory activities before boarding after the last train arrives at station D. We assume that a fixed time is needed to complete the preparatory activities, which is long enough before boarding (e.g., 1.5 h). In addition, it is uncommon for the passenger to arrive too early. There may be an upper bound time (e.g., 2.5 h for domestic air transport trips) for early arrival to avoid overlong waiting. Therefore, with a valid time range (1.5–2.5 h in the above example) after the passenger's arrival, we can analyze the potential coordination between the last trains and the connecting flights. The flight passenger volume covered by the time range after the last train's arrival at station D (the red shadow in Fig. 4) can reflect the coordination of the last train's arrival time. Similarly, in the opposite direction of Route 2, an ordinary air transport passenger may have a range of time expense at station D before accessing the URT (the blue shadow in Fig. 4). Taken together, we are able to analyze the potential coordination between the two modes.

The coordination function is complicated since the space-time distribution of the connecting modes does not have a fixed pattern as seen in Fig. 1. We propose an approximation approach to describe the coordination function in the discrete time domain. The time within range  $[t_1^0, t_1^E]$  is equally discretized into time intervals with  $\delta$  as the length of one interval. A parameter,  $f_{jl^1s^1m^1}^{y,i}$ , is introduced to represent the coordination quantity at each time interval, which can be calculated below in advance. Let  $y$  denote the coordination type:  $y = 0$  represents the coordination of the arrival of the last train with another mode's departure and  $y = 1$  represents the opposite.  $j$  denotes the beginning time at the  $j$ -th time interval.  $J_{il^1s^1m^1}$  denotes the set of  $j$  on direction  $m^1$  of line  $l^1$  at stations<sup>1</sup> of mode  $i$ . When the valid time ranges are given, the coordination is determined by the beginning time. With other notations unchanged, we indicate the total coordination quantity  $f_{jl^1s^1m^1}^{y,i}$  across  $\forall j$  using 0–1 variable  $x_{jl^1s^1m^1}^{y,i}$  as

$$f_{jl^1s^1m^1}^{y,i} = \sum_{j \in J_{il^1s^1m^1}} x_{jl^1s^1m^1}^{y,i} f_{jl^1s^1m^1}^{y,i} \quad (14)$$

$$\sum_{j \in J_{il^1s^1m^1}} x_{jl^1s^1m^1}^{y,i} = 1 \quad (15)$$

where  $f_{jl^1s^1m^1}^{y,i}$  is the pre-calculated time-dependent coordination quantity for mode  $i$  at  $j$ -th time interval in coordination type  $y$  of the last train in direction  $m^1$  of line  $l^1$  at  $s^1$ .  $x_{jl^1s^1m^1}^{y,i}$  is a 0–1 variable,  $x_{jl^1s^1m^1}^{y,i} = 1$  when the successful coordination for mode  $i$  at  $j$ -th time interval in coordination type  $y$  of the last train in direction  $m^1$  of line  $l^1$  at  $s^1$ ; otherwise,  $x_{jl^1s^1m^1}^{y,i} = 0$ .

The relationship between  $x_{jl^1s^1m^1}^{y,i}$  and arrival time or departure time of the last train is formulated as

$$t_{jl^1s^1m^1}^{y,i} = t_1^0 + \delta \cdot \sum_{j \in J_{il^1s^1m^1}} j \cdot x_{jl^1s^1m^1}^{y,i} \quad (16)$$

$$t_{jl^1s^1m^1}^{0,i} = a_{jl^1s^1}^m \quad (17)$$

$$t_{jl^1s^1m^1}^{1,i} = d_{jl^1s^1}^m \quad (18)$$

where  $t_{jl^1s^1m^1}^{0,i}$  and  $t_{jl^1s^1m^1}^{1,i}$  an intermediate variable that represents the arrival time ( $a_{jl^1s^1}^m$ ) and departure time ( $d_{jl^1s^1}^m$ ) of the last train in direction  $m^1$  of line  $l^1$  at station  $s^1$  respectively. With the formulated coordination quantity, we use  $w_{il^1s^1}$  to indicate the importance

coefficient of station  $s^1$  of line  $l^1$  in mode  $i$ .

In Model 3, a new objective,  $P_3$ , to maximize the coordination quantity for all modes is formulated as

$$\text{Max } P_3 = \sum_{\Omega_4} w_{il^1s^1} f_{[l^1s^1m]}^{v,i} \quad (19)$$

$$\Omega_4 = \{i, s^1, l^1, m^1, y | i \in I, s^1 \in R(i), l^1 \in H(s^1), m^1 \in M, y \in Y\}$$

Combining  $P_2$  and  $P_3$ , we use a linear weighting method to convert the bi-objective to a single objective as

$$\text{Max } P = \alpha_2 \cdot \frac{(P_2 - P_2^{\min})}{(P_2^{\max} - P_2^{\min})} + \alpha_3 \cdot \frac{(P_3 - P_3^{\min})}{(P_3^{\max} - P_3^{\min})} \quad (20)$$

where  $\alpha_2$  and  $\alpha_3$  represent the weights of the objectives with  $\alpha_2 + \alpha_3 = 1$  for normalization.

The constraints are summarized as

*st.3* { Eqs.(2) – (5), (10) – (11), (13)  
 Eqs.(14) – (18)

Overall, inheriting the character of Model 2, Model 3 still remains in the form of mixed-integer programming. Moreover, Model 3 further considers the space-time distribution of the arrivals and departures of the connecting modes. Therefore, Model 3 achieves one-to-many (the last train- to -many arrivals and departures of the connecting modes) instead of one-to-one (last train- to one arrival or departure of the connecting modes) transferability at transfer stations between different transport modes. This is a novel view to improve multimodal coordination, which is seldom found in existing studies.

### 2.5. Model analysis

Linearization techniques are employed in Models 1, 2, and 3 for finding the exact optimal solutions. First, the space-time con-

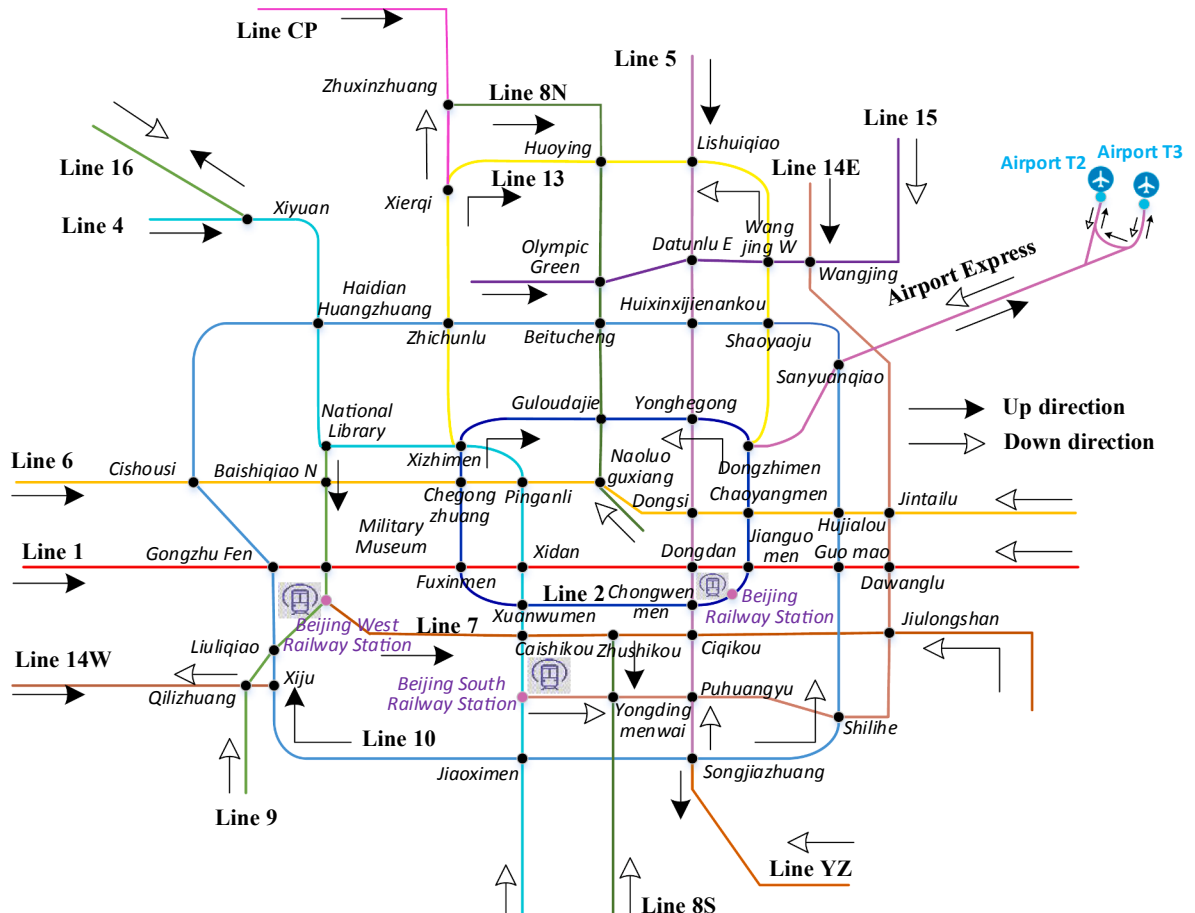


**Fig. 5.** The network of Beijing urban transit.

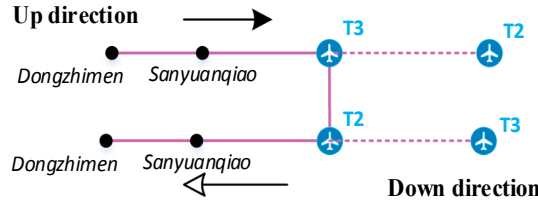
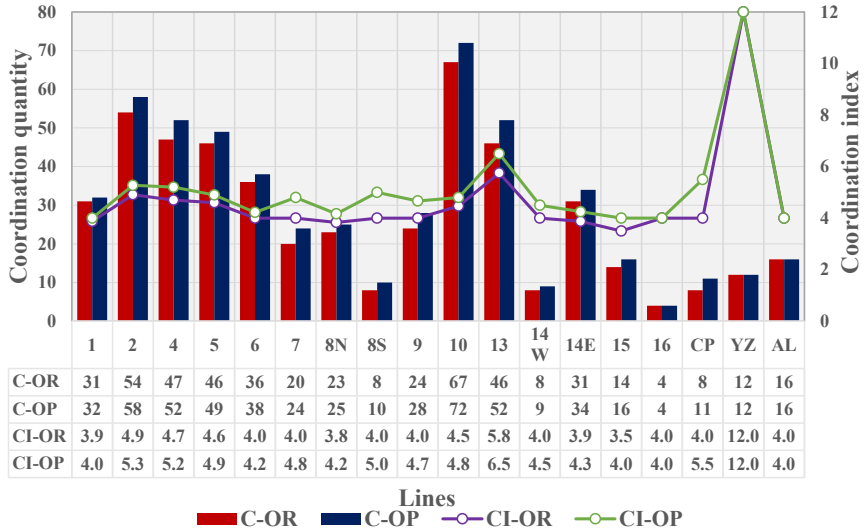


Fig. 6. Illustration of Airport Express.



C-OR: coordination-original, C-OP: coordination-optimized, CI-OR:CI-original, CI-OP: CI-optimized.

Fig. 7. Improvements of coordination in different lines.

straints are linearized by the Big M method (Kang and Meng, 2017) in Model 1. By introducing new variables and the Big M method, objective  $P_2$  in Model 2 is linearized. Meanwhile, objective  $P_1$  is converted into a constraint. Finally, time is discretized and the time constraints of coordination are linearized. A linear weighting method (Gunantara, 2018) is further utilized to convert the bi-objective to a single objective. In summary, all objective functions are specified in MILP formulations, which can be solved by existing optimization solvers (e.g., Cplex or Gurobi).

### 3. Case study

In this section, the URT network in Beijing is employed to validate the effectiveness of the proposed models. Note that, each line is divided into two different sub-lines by the up- and down-directions (for instance, subway Line-1 “sline1” includes “sline1up” and “sline1down”). As shown in Fig. 5, each URT line is marked with two distinctive running directions. The stations are numbered in Table A1. Line and station characteristics are given in Table A2. The travel time from the starting (first) station to station  $s$  in direction  $m$  on line  $l$  ( $r_{ls}^m$ ,  $\forall l, s, m$ ) can be found in Table A3. (Table A1-3 are given in the appendix.).

The Airport Express is a special line in y-shape without the clear up-direction or down-direction. To make it consistent with other lines, we divide the Airport Express in two directions by introducing dummy stations. As shown in Fig. 6, the route (Dongzhimen → Sanyuanqiao → T3 → T2) from left to right is in the up-direction, and the other way round is in the down-direction.

Suppose the planning horizon of the last trains begins at 21:00 on an average day. The original departure times of different lines are listed in Table A4 in the appendix. For the sake of convenience, we set 21:00 as the beginning time 0 in the analysis.

The MILP models are solved by Python and Gurobi in a personal computer (8G RAM and Inter Core i7-6700U CPU), which can find the exact optimal solutions within 3 minutes. We illustrate below the running results of the three models in three cases respectively.

#### 3.1. Case 1 for model 1

To test the improvement of coordination within the URT network, we set a 15 min buffer time to allow departure time variations at the starting station. That variation may also result in changes in the departure times at other stations, constrained within  $\pm 15$ mins. We calculate a coordination index (CI) for each line, equal to the coordination quantity (C) divided by the total number of transfer stations

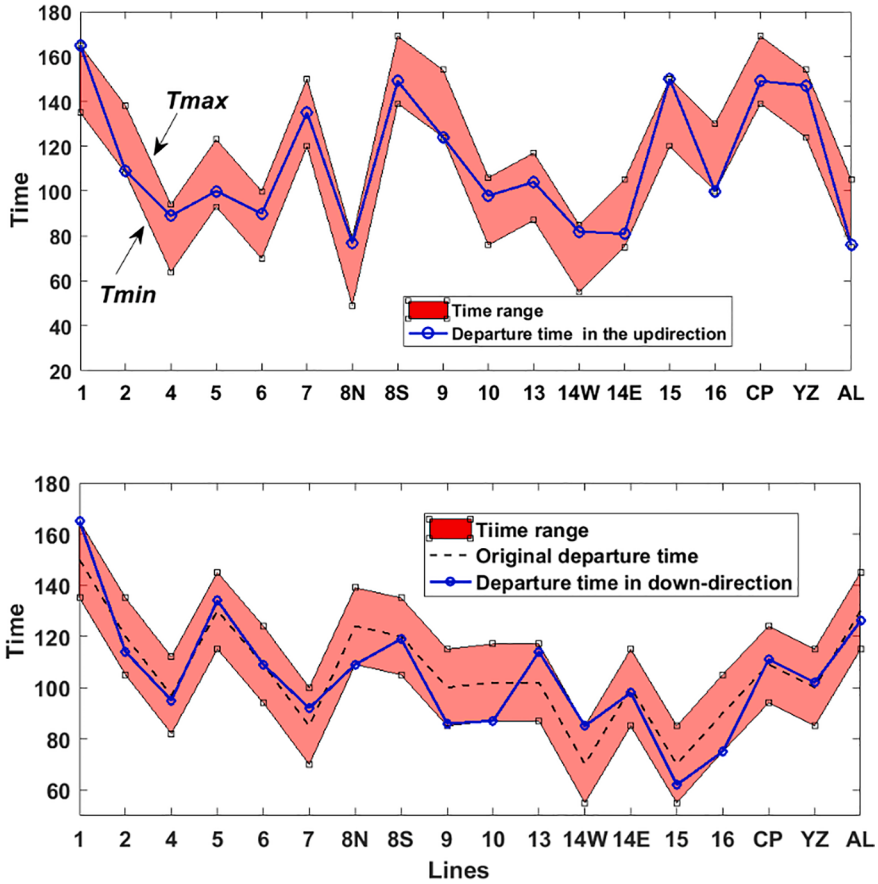


Fig. 8. Comparison between the optimized and original departure time.

Improvements for the coordination between different lines																		
Lines	sline1	sline2	sline4	sline5	sline6	sline7	sline8N	sline8S	sline10	sline13	sline14W	sline14E	sline15	sline16	slineCP	slineYZ	slineAL	
sline1	0	0	0	0	0	0	0	0	0	0	0	0	0	0	0	0	0	
sline2	0	0	0	0	0	0	0	0	0	0	0	0	0	0	0	0	0	
sline4	0	0	-2	0	0	0	0	0	0	0	0	0	0	0	0	0	0	
sline5	0	0	-2	0	0	0	0	0	0	0	0	0	0	0	0	0	0	
sline6	0	0	-2	0	0	0	0	0	0	0	0	0	0	0	0	0	0	
sline7	0	0	0	0	0	0	0	0	0	0	0	0	0	0	0	0	0	
sline8N	0	0	-1	0	0	0	0	0	0	0	0	0	0	0	0	0	0	
sline8S	0	0	0	0	0	0	0	0	0	0	0	0	0	0	0	0	0	
sline9	0	0	0	0	0	0	0	0	0	0	0	0	0	0	0	0	0	
sline10	0	0	0	0	0	0	0	0	0	0	0	0	0	0	0	0	0	
sline13	0	0	0	0	0	0	0	0	0	0	0	0	0	0	0	0	0	
sline14W	0	0	0	0	0	0	0	0	0	0	0	0	0	0	0	0	0	
sline14E	0	0	0	0	0	0	0	0	0	0	0	0	0	0	0	0	0	
sline15	0	0	0	0	0	0	0	0	0	0	0	0	0	0	0	0	0	
sline16	0	0	0	0	0	0	0	0	0	0	0	0	0	0	0	0	0	
slineCP	0	0	0	0	0	0	0	0	0	0	0	0	0	0	0	0	0	
slineYZ	0	0	0	0	0	0	0	0	0	0	0	0	0	0	0	0	0	
slineAL	0	0	0	0	0	0	0	0	0	0	0	0	0	0	0	0	0	

✗  $z_0$  : Reduction in coordination,  $z_0 < 0$ .  
■  $z_1$  : Remain unchanged in the coordination,  $z_1 = 0$ .  
✓  $z_2$  : Growth in coordination,  $z_2 > 0$ .

Fig. 9. Improvements of coordination between different lines in detail.

(NS), i.e.,  $CI = \frac{C}{NS}$ . The CI reflects the average coordination level of a URT line. The improvements of coordination in different lines are shown in Fig. 7. The coordination of most lines is improved, except Line 16, Airport Express, and Line YZ. The total coordination quantity is 252 for the optimized timetable, which is increased by 10% compared with the original (229). The optimized departure times of the last trains at the starting stations are shown in Fig. 8. As seen, the optimized departure times are different from the original ones. However, for most lines, the deviations from the original one are less than 15 min, meaning that slight changes in departure times

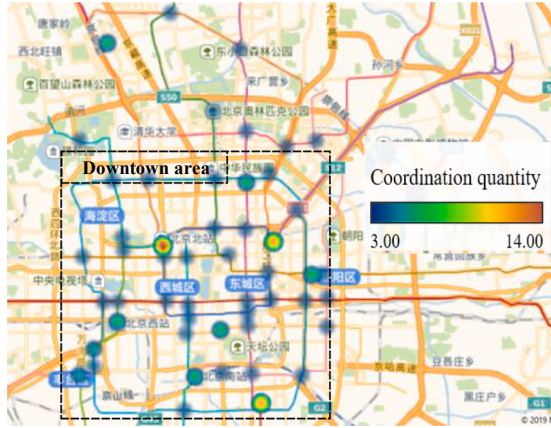


Fig. 10. Quantity distribution of coordination on the network.



Fig. 11. Improvement of coordination on the network.

lead to much improvement.

The improvements of coordination between different lines are shown in Fig. 9. With the optimized timetable, it is easier to transfer between different lines except for Lines 2 or 10, which are loop lines with several transfer stations and still high accessibility to other lines. That is to say, the reduction of coordination in these two lines has little influence on the connectivity of the URT network but more positive effects on the coordination of other lines.

Fig. 10 shows the spatial distribution of the coordination of the optimized timetable. Just as the thermodynamic diagrams, the depth of the color at a station means the connection level. The warmer the color is, the better coordination a station has. It can be seen that the coordination is evenly distributed in the URT network. The improvement reflected by the size of the circle at each station is shown in Fig. 11. There is only one station (Dongsi, shown by the green circle) with reduced coordination. Therefore, Model 1 is effective in raising the coordination among the last trains in the URT network.

### 3.2. Case 2 for model 2

We consider two connecting modes to the URT network, namely, railway and airplane, as shown in upper-right and lower-left corners of Fig. 12. We have  $i \in I = \{1, 2\}$  and set  $i = 1$  for airplane and  $i = 2$  for the railway. The first-layer stations and lines of the two modes are listed in Table 1. There are five lines directly connecting the railway stations and only one line (Airport Express) connecting the airport. To clearly trace the improvement, we divide the objective of Model 2 ( $P_2$ ) into two parts:  $P_{2-1}$  and  $P_{2-2}$ .  $P_{2-1}$  denotes the coordination serving passengers who access the connecting modes.  $P_{2-2}$  indicates the coordination of serving passengers who egress the connecting modes. Thus, we have Eqs. (21) and (22).

$$P_{2-1} = \sum_{\Omega_2} \theta_{l^1 l^2 s^2}^{m^1 m^2} \quad (21)$$

$$P_{2-2} = \sum_{\Omega_2} \theta_{l^1 l^2 s^2}^{m^1 m^2} \quad (22)$$

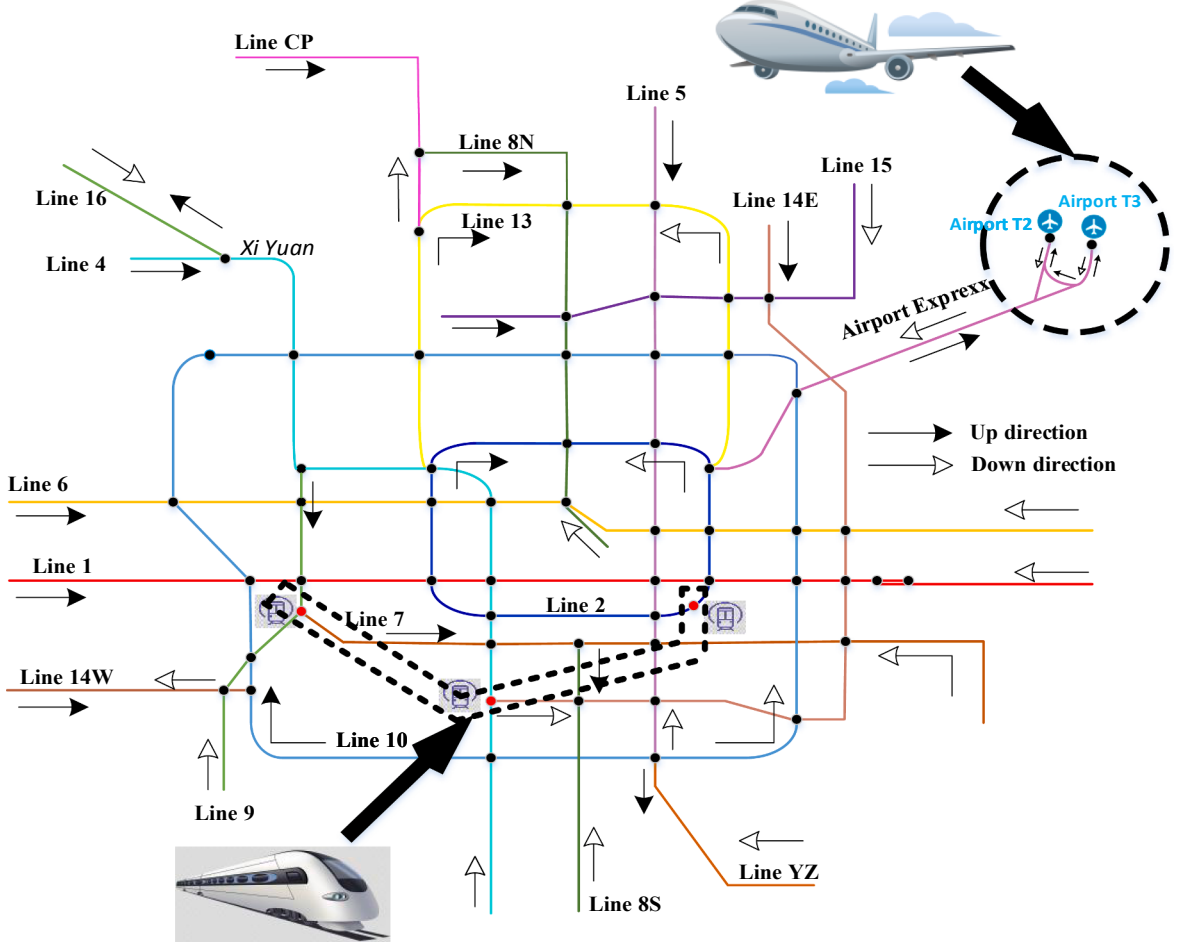


Fig. 12. Distribution of mode on the network.

**Table 1**  
The compositions of the railway mode and airplane mode.

	Mode	First-layer station	First-layer line
1	Railway	Beijing Railway Station Beijing Railway South Station Beijing Railway Western Station	Line 2 Line 4, Line 14E Line 7, Line 9
2	Airplane	Airport T2 Airport T3	Line AL

The importance coefficient for the railway and airplane modes are set the same in this case, i.e., considering undifferentiated passengers, i.e.,  $w_1 = w_2 = 1$  in Eq. (6).

The outcomes of  $P_2$  are shown in Fig. 13 with the varying proportion ( $\alpha$ ) of the maximum coordination of the whole network.  $P_{2-1}$  is improved to the maximum value when  $\alpha$  is decreased from 1 to 0.97. However,  $P_{2-2}$  has nearly the opposite trend.  $P_2$  on the whole is improved to a maximum value when  $\alpha$  is decreased from 1 to 0.97. When  $\alpha \leq 0.95$ , all the outcomes are flat. However, a slight reduction in  $P_1$  ( $252-248 = 4$ ) is associated with more coordination for the railway and airplane modes. The maximum growth is 42% (or  $(1575-1118)/1118 *100\%$ ), where 1575 and 1118 are the optimized and original  $P_2$  respectively.

We summarize the results in six indices ( $h_1, h_2, h_3, h_4, h_5, h_6$ ) to show the detailed improvement of the optimized timetable over the original one.

We consider the “coordination index of the line (CIL)” for a mode calculated by the coordination quantity of the mode (CQ) divided by the total number of the first-layer line for this mode (NLM), i.e.,  $CIL = \frac{CQ}{NLM}$ . The numbers of the first-layer lines of the railway and airplane modes are five and one respectively. The optimized results are shown in Table 2. In detail, the following results are found.

(1) The coordination quantity of the railway mode is improved more than that of the airplane mode ( $371 > 86$ ,  $42.8\% > 34.1\%$ ). However, as for the coordination index, coordination for the airplane mode is enhanced more than that for the railway mode ( $86 > 74.2\%$ ).

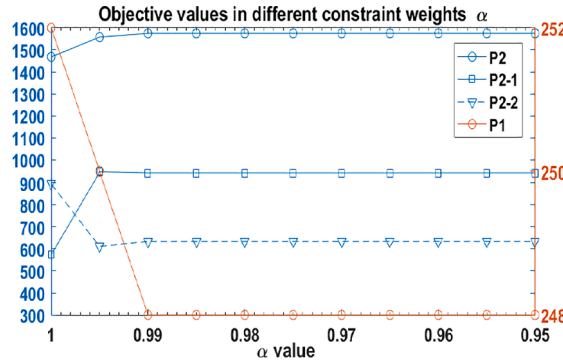


Fig. 13. Objective values in different constraint weights  $\alpha$  in Model 2.

Table 2

Improvements for the coordination of the railway mode and airplane mode ( $h_1$ ).

Objective	Mode	Railway mode	Airplane mode
$P_{2-1}$	Original	285	110
	Optimized	450	184
	Improvement	165	74
	Ratio (%)	<b>57.8</b>	<b>67.2</b>
$P_{2-2}$	Original	581	142
	Optimized	787	154
	Improvement	206	12
	Ratio (%)	<b>35.5</b>	<b>8.4</b>
$P_2$	Original	866	252
	Optimized	1237	338
	Improvement	371	86
	Ratio (%)	<b>42.8</b>	<b>34.1</b>
Number of the first-layer line		5	1
Coordination index of the line	Original	173.2	252
	Optimized	247.4	338
	Improvement	74.2	86
	Ratio (%)	<b>42.8</b>	<b>34.1</b>

Table 3

Improvements for the coordination in the first-layer station ( $h_2$ ).

Objective	Station	58	59	14	24	38
$P_{2-1}$	Original	55	55	129	73	83
	Optimized	92	92	186	152	112
	Improvement	37	37	57	79	39
	Ratio (%)	<b>67.3</b>	<b>67.3</b>	<b>44.2</b>	<b>108.2</b>	<b>34.9</b>
$P_{2-2}$	Original	71	71	128	323	71
	Optimized	77	77	177	410	77
	Improvement	6	6	59	87	6
	Ratio (%)	<b>8.5</b>	<b>8.5</b>	<b>38.5</b>	<b>38.3</b>	<b>53.8</b>
$P_2$	Original	126	126	257	396	213
	Optimized	169	169	363	562	312
	Improvement	43	43	106	166	99
	Ratio (%)	<b>34.1</b>	<b>34.1</b>	<b>41.2</b>	<b>41.9</b>	<b>46.5</b>

$P_{2-1}$  has a high improvement than  $P_{2-2}$ , implying it is easier to access than to egress the railway station/airport by the last trains of URT.

(2) Stations 58 (Airport T2) and 59 (Airport T3) are two first-layer stations of the airplane mode, belonging to the same line (Airport Express). Therefore, the valid coordination for stations 58 and 59 is the same as shown in Table 3. It is obvious that the improvements for the stations belonging to the railway mode are higher. This is coincident with the fact that each station in the railway mode belongs to more than one URT line. The results also show that improvement for  $P_{2-1}$  is much higher than that for  $P_{2-2}$ .

(3) Fig. 14 shows the geographical distribution of the first-layer lines (thickened and colored lines). The railway mode covers more lines (Line 2, 4, 7, 9, 14E) and more widely distributed. The detailed improvements are listed in Table 4. The improvement for  $P_{2-1}$  is

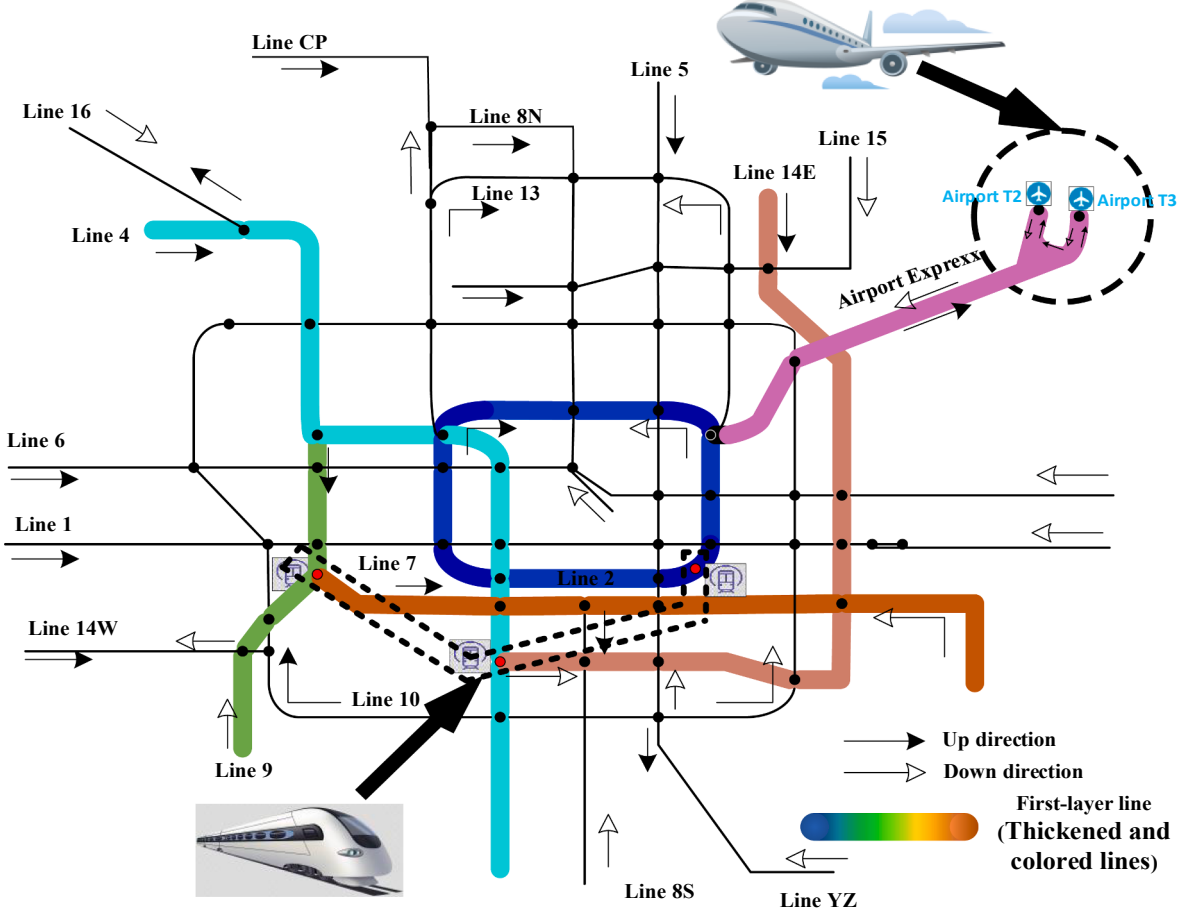


**Fig. 14.** Geographical distribution of the first-layer line.

**Table 4**  
Improvements for the coordination in the first-layer line ( $h_3$ ).

Objective	First-layer line	SlineAL	Sline2	Sline4	Sline14E	Sline7	Sline9
$P_{2-1}$	Original	110	129	65	8	38	45
	Optimized	184	186	105	47	23	89
	Improvement	74	57	40	39	-15	44
	Ratio (%)	67.2	44.2	61.5	487.5	-39.5	97.8
$P_{2-2}$	Original	142	128	205	118	56	74
	Optimized	154	177	269	141	100	100
	Improvement	12	49	64	23	44	26
	Ratio (%)	8.5	38.3	31.2	19.5	78.6	35.1
$P_2$	Original	252	257	270	126	94	119
	Optimized	338	363	374	188	123	189
	Improvement	86	106	104	62	29	70
	Ratio (%)	34.1	41.2	38.5	49.2	30.9	58.8
Number of second-layer station		2	10	10	8	5	6
Ratio of average improvement (%)		17.1	4.1	3.9	6.2	6.2	9.8

generally higher than that for  $P_{2-2}$  except for Line 7. Also, the coordination of Line 7 is the only one that decreases by nearly 40%. On the whole, the improvement for each first-layer line is over 30%. Sline9 has the greatest improvement (60% or so). However, the average improvement from the second-layer stations is much higher in Airport Express than in other lines, implying an efficient connection between Airport Express and the URT network.

(4) Fig. 15 shows the improvements of the coordination in the second-layer stations in. Although the performances for the second-layer stations are uneven, most stations have improvements in  $P_2$ .

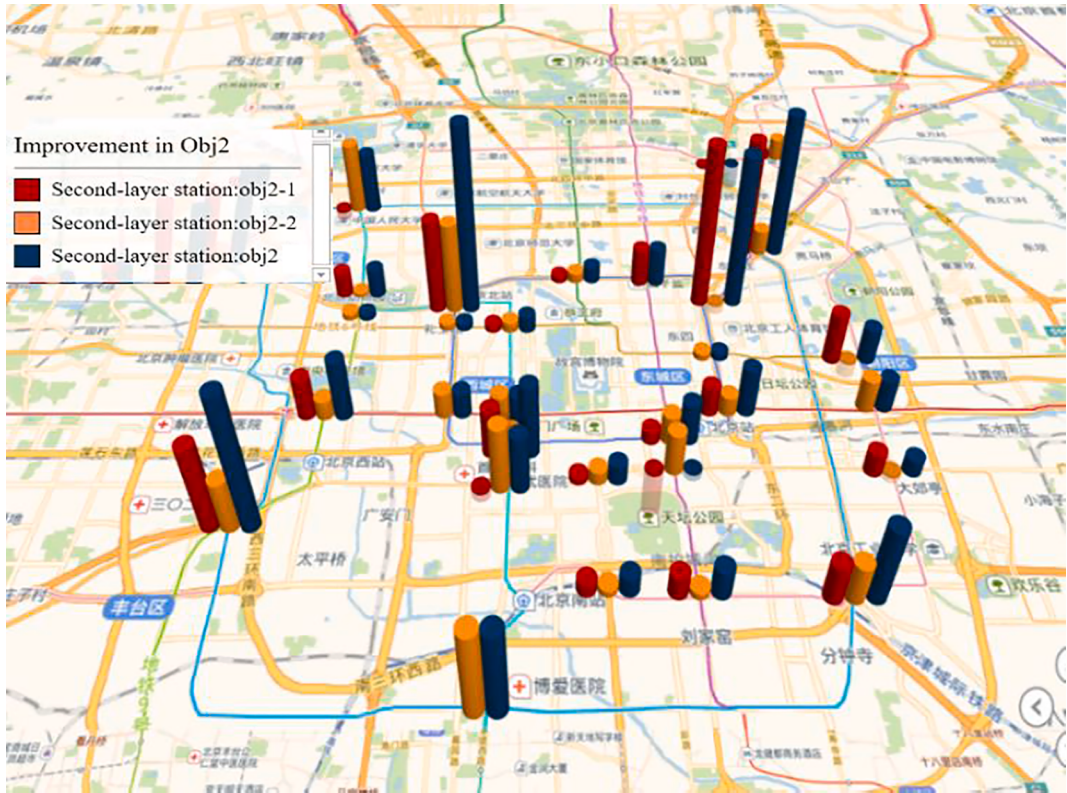


**Fig. 15.** Improvements of the coordination in the second-layer station ( $h_4$ ).

There are several second-layer stations showing negative growth in  $P_{2-1}$  or  $P_{2-2}$ . However, we find that the stations with higher importance for the railway and airplane modes achieve remarkable improvements as shown in Fig. 16. The improvement is shown in a cluster distribution with six groups in line with the geographical distribution of the first-layer lines.

(5) As for the improvements of the coordination in the second -layer line, similar to the first-layer lines, the growths are generally positive except for Line 7. Also, the improvement of  $P_{2-1}$  is generally higher than that of  $P_{2-2}$ .

(6) The original and optimized coordination between different lines are shown in Fig. 17 (a)-(b). The width of the arc represents the coordination between different lines: the wider an arc is, the higher coordination a line has with other lines. The more coordination between two lines, the thicker arcs connecting the two lines are in the figures. It can be seen that the coordination between different lines is improved with more and thicker arcs.

### 3.3. Case 3 for model 3

We take into account the space-time distribution of arrivals and departures of trains and flights. For the airplane passengers, we suppose that the duration for preparatory activities before boarding is longer than 1.5 h and the buffer time for arriving early is 1 h. Therefore, the valid coordination quantity related to arrival involves time window [1.5 h, 2.5 h] after passengers' arrivals. Similarly, suppose the valid coordination quantity related to departure involves time window [0.5 h, 1 h]. Since it usually takes less time for railway passengers to board the trains. The corresponding time windows related to arrival and departure are [1 h, 2 h] and [0.5 h, 1 h] respectively for railway passengers.

We set the time window for the last train coordination at the first-layer stations is [10:00 pm, 12:00 pm], making,  $t_{lm}^O = 60$ ,  $t_{lm}^E = 180$  and  $j \in [0, 120]$  in our analysis. Figs. 18-19 show the coordination quantity of the railway stations and airport terminals at each time interval. As the number of arrival/departure trains at the railway stations is less than that at the airport in the evening in Beijing, the coordination quantity of the railway station is generally less than that of the airport. The maximum coordination related to arrival and departure are listed in Table 5. Normally, there are few trains departing after 10:00 pm. The maximum coordination related to arrival at Beijing South is much lower than others. we set  $\alpha = 0.9$  in Case 3 with a reference to Case 2, where all indicators are unchanged if  $\alpha \leq 0.9$ .

Considering no difference among the first-layer stations,  $w_{il^1s^1}$  is set as 1. To reveal the influence of different weighing parameters, we

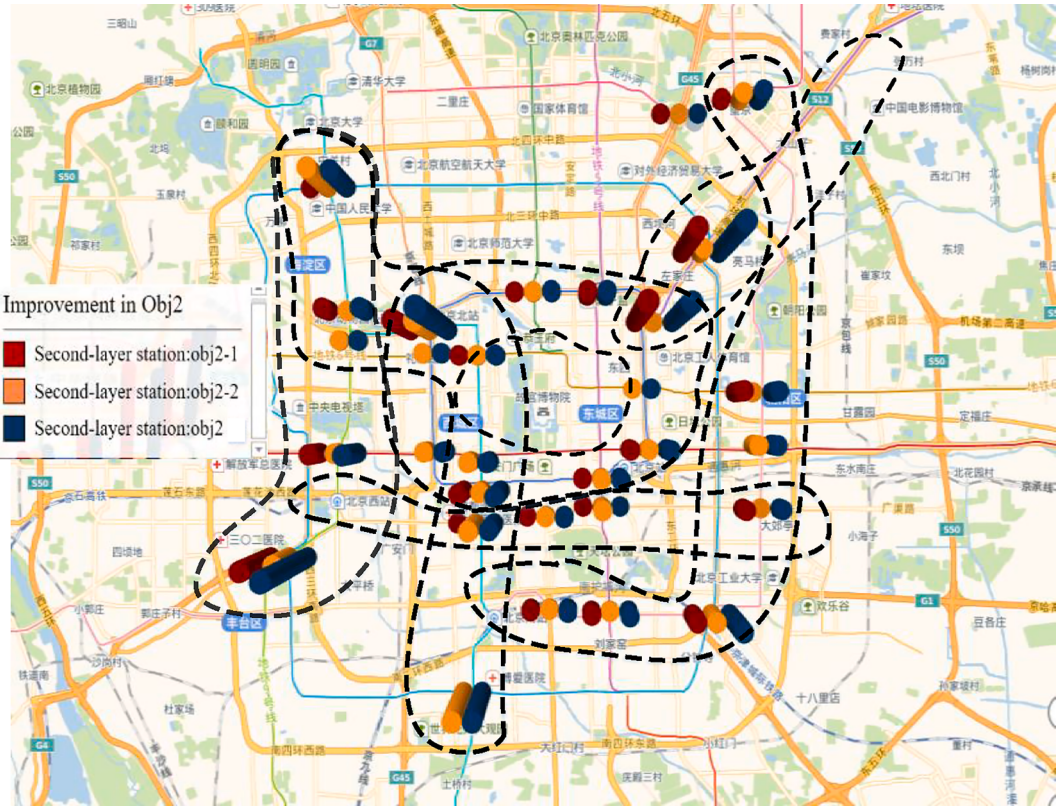


Fig. 16. Cluster distribution of the coordination in the second-layer stations.

Original coordination between different lines      Optimized coordination between different lines

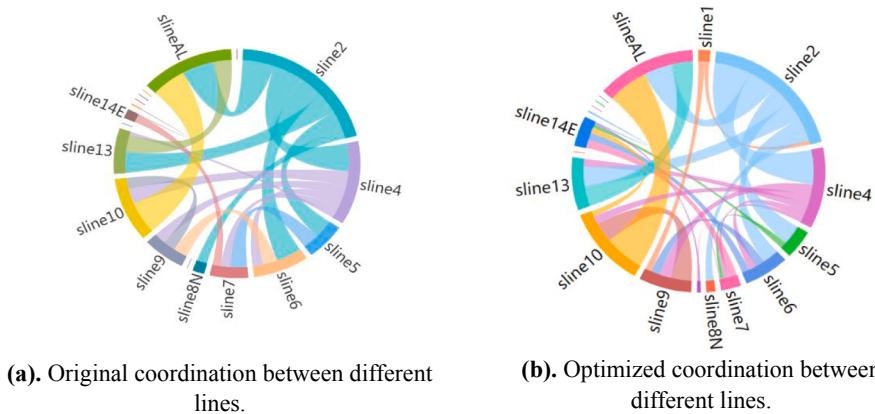


Fig. 17. Improvements for the coordination between different lines ( $h_6$ ).

set variant weights with a common difference of 0.1. Table 6 shows the results with different  $\alpha_2$  and  $\alpha_3$ . We can see that  $P_1, P_2, P_{2-1}, P_{2-2}$  increase with rising  $\alpha_2$ . The objectives  $P_2$  and  $P_3$  with varying weights are shown in Fig. 20.  $P_3$  decreases rapidly when  $\alpha_2 \geq 0.8$ . Therefore, when  $\alpha_2 = 0.8$ , a compromise solution is found in this example. Similarly, we divide  $P_3$  into two parts:  $P_{3-1}$  and  $P_{3-2}$ . The former denotes the coordination serving passengers for accessing (coordination related to arrival), while the latter indicates the coordination serving passengers for egressing (coordination related to departure). When  $\alpha_2 = 0.8$ ,  $P_3$  is improved by 22 (or 154–132). We summarize the results in three indices ( $u_1, u_2, u_3$ ) to show the detailed improvements of the optimized timetable over the original one.

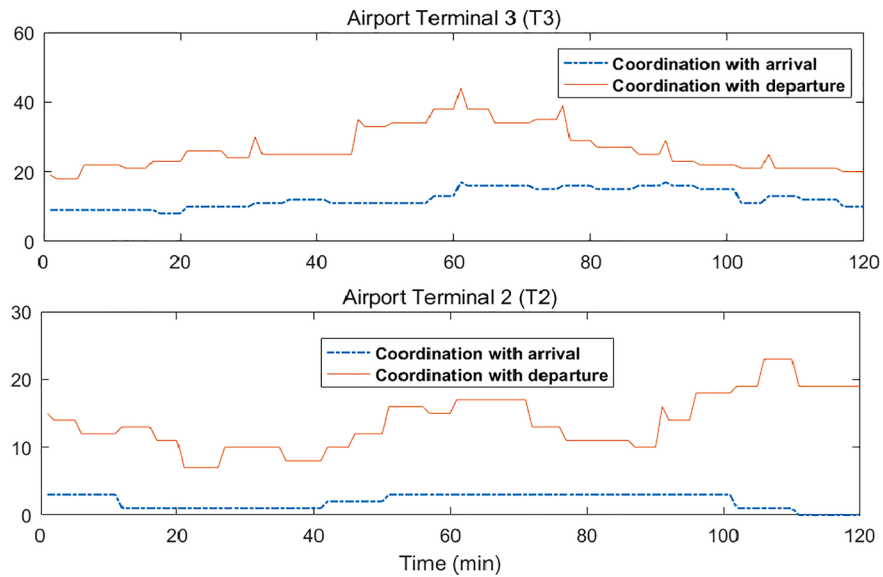


Fig. 18. Coordination quantity of the airport terminals at each timestamp.

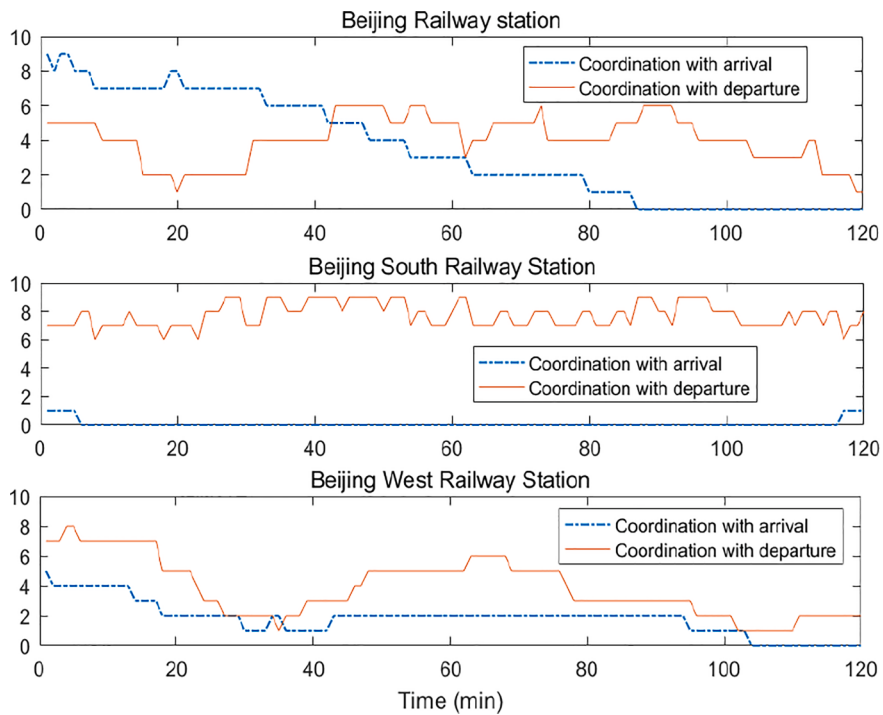


Fig. 19. Coordination quantity of the railway stations at each timestamp.

Table 5

Maximum coordination.

Stations	T3	T2	Beijing	Beijing South	Beijing West
Maximum coordination related to arrival	3	17	9	1	5
Maximum coordination related to departure	28	44	6	9	8

**Table 6**  
Objectives under different weights.

$\alpha_2$	$\alpha_3$	$P_2$	$P_{2-1}$	$P_{2-2}$	$P_3$	$P_1$
0	1	1023	458	565	158	227
0.1	0.9	1459	569	890	158	245
0.2	0.8	1459	569	890	158	246
0.3	0.7	1459	569	890	158	246
0.4	0.6	1459	569	890	158	246
0.5	0.5	1459	569	890	158	246
0.6	0.4	1459	569	890	158	246
0.7	0.3	1459	569	890	158	246
0.8	0.2	1525	609	916	154	244
0.9	0.1	1555	607	948	143	248
1	0	1575	634	941	118	248

We also consider the “coordination index of the station (CIS)” for a mode, equal to the coordination quantity of the mode (CQ) divided by the total number of the first-layer station for this mode (NSM), i.e.,  $CIS = \frac{CQ}{NSM}$ . As shown in Table 7, the improvements of the CI are 17.9% and 15.5% for the railway mode and airplane mode respectively. The railway mode has no improvement in  $P_{3-1}$ , while the coordination for the airplane mode is raised by 42.9%. However, the railway mode has more improved coordination than the airplane mode in  $P_{3-2}$  (21.1% > 7.8%). Overall, the railway and airplane modes have comparable improvements in  $P_3$ . The improvements of  $P_3$  in the first-layer stations are listed in Table 8. Since T2 (station 59) is the terminal station and the maximum coordination related to arrival is 3, there is no room for improvement in  $P_{3-1}$ . Only T3 (station 58) has an improvement in  $P_{3-1}$ . All stations have improved coordination above 20% in  $P_{3-2}$  except for T2 (station 59). Although T2 has a reduction by 30% in  $P_3$ , the coordination reduction is 6, a small number compared to the total of  $P_3$  (154). In general, Model 3 has improved coordination in the

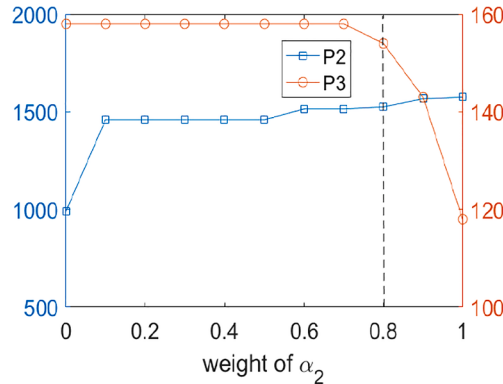


Fig. 20. Objectives of Model 3 vary with different  $\alpha_2$ .

**Table 7**  
Improvements of  $P_3$  of the railway and airplane modes ( $u_1$ ).

Objective	Mode	Airplane mode	Railway mode
$P_{3-1}$	Original	14	10
	Optimized	20	10
	Improvement	6	0
	Ratio (%)	<b>42.9</b>	<b>0</b>
$P_{3-2}$	Original	51	57
	Optimized	55	69
	Improvement	4	12
	Ratio (%)	<b>7.8</b>	<b>21.1</b>
$P_3$	Original	65	67
	Optimized	75	79
	Improvement	10	12
	Ratio (%)	<b>15.4</b>	<b>17.9</b>
Number of the first-layer station		2	3
Coordination index of the station	Original	32.5	22.3
	Optimized	37.5	26.3
	Improvement	5	4
	Ratio (%)	<b>15.4</b>	<b>17.9</b>

**Table 8**  
Improvements for the  $P_3$  in the first-layer station ( $u_2$ ).

Objective	Station	58	59	14	24	38
$P_{3-1}$	Original	11	3	2	0	8
	Optimized	17	3	2	0	8
	Improvement	6	0	0	0	0
	Ratio (%)	<b>54.5</b>	<b>0</b>	<b>0</b>	<b>0</b>	<b>0</b>
$P_{3-2}$	Original	34	17	9	30	18
	Optimized	44	11	11	36	22
	Improvement	10	-6	2	6	6
	Ratio (%)	<b>29.4</b>	<b>-18.5</b>	<b>22.2</b>	<b>20</b>	<b>22.2</b>
$P_3$	Original	45	20	11	30	26
	Optimized	61	14	13	36	30
	Improvement	16	-6	2	6	4
	Ratio (%)	<b>35.5</b>	<b>-30</b>	<b>18.2</b>	<b>20</b>	<b>15.4</b>

**Table 9**  
Improvements of  $P_3$  in the first-layer lines ( $u_3$ ).

Objective	First-layer line	SlineAL	Sline2	Sline4	Sline14E	Sline7	Sline9
$P_{3-1}$	Original	14	2	0	0	4	4
	Optimized	20	2	0	0	4	4
	Improvement	6	0	0	0	0	0
	Ratio (%)	<b>42.9</b>	<b>0</b>	<b>0</b>	<b>0</b>	<b>0</b>	<b>0</b>
$P_{3-2}$	Original	51	9	14	16	10	8
	Optimized	55	11	18	18	12	10
	Improvement	4	2	4	4	2	2
	Ratio (%)	<b>7.8</b>	<b>22.2</b>	<b>28.6</b>	<b>12.5</b>	<b>20</b>	<b>25</b>
$P_3$	Original	65	11	14	16	14	12
	Optimized	75	13	18	18	16	14
	Improvement	10	2	4	2	2	2
	Ratio (%)	<b>17.2</b>	<b>18.2</b>	<b>38.5</b>	<b>28.6</b>	<b>14.3</b>	<b>16.7</b>

terminal stations. T3 (station 58) has the biggest  $P_3$ . Therefore, it is claimed that the last train of Airport Express provides a good connection to the airport. The improvements of  $P_3$  in the first-layer lines are listed in Table 9. Only the Airport Express (SlineAL) has an improvement with a high ratio (42.9%) in  $P_{3-1}$ .  $P_{3-2}$  is improved the most in Line 4 (Sline4) by 28.6% and the least in Airport Express by 7.8%. For the improvements in  $P_3$ , Airport Express has the most improvement in coordination number (10), while Line 4 has the most growth in proportion (38.5%). As a whole, every line has an average improvement above 15%.

To test the sensitivity of buffer time, we conduct a group of tests. The results are shown in Fig. 21. It is clear that the objectives ( $P_1$ ,  $P_2$ ,  $P_3$ ) increase with the growth of the buffer time. However, the growth rates of the objectives reduce with bigger buffer times. Therefore, the improvement for the objectives may not be infinite. As seen, the buffer time of 15 min is well-selected in the above analysis.

All in all, Cases 1, 2, and 3 have sufficiently validated Models 1, 2, and 3. The models are effective in improving the coordination of the last trains. Model 1 has raised the transferability at transfer stations by 10%. Model 2 has promoted the coordination with the railway and airplane modes by 42.8% and 34.1 respectively. Taking into account the space–time distribution of the arrival and departure of the

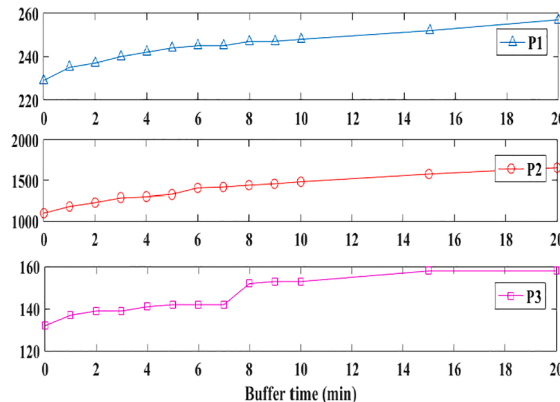


**Fig. 21.** Objectives vary with different buffer times of the time window.

trains and flights, Model 3 has increased the valid coordination at terminal stations for the railway and airplane modes by 17.9% and 15.4% respectively. Moreover, the sensitivity of parameters in the models is analyzed to enhance the performance of the models.

#### 4. Conclusions and future work

The timetabling of the last trains in a URT network is a challenging topic. Considering the coordination with the connecting modes, this paper suggests three models in progressive relationship to optimize the last train timetable. Based on a basic model (Model 1), Models 2 and 3 take into account the valid transferability at transfer stations, which can not only achieve the accessibility of the DR-LTTP proposed by Zhou et al., (2019), but also consider passenger paths with reduced complexity. All the modes are in the form of mixed-integer linear programming (MILP) by a series of linearizing techniques, and thus can be readily solved by existing optimization solvers.

The proposed models have been tested on the Beijing URT network, which connects three railway stations and two airport terminals. Significant improvements are obtained at both the station-level and line-level ( $P_1, P_2, P_3$ ) after optimization. Especially, Model 3 has large improvement in connecting the Airport Express, compared with Model 2, implying that it is much important to optimize the last train timetable incorporating the temporal pattern of the connecting modes.

Further research can be extended in the following aspects. First, the robustness of the last train timetable of the URT network should be considered. The arrival and departure times of the train/flight at the railway stations and airports vary on different days. Designing a robust timetable that fits different scenarios has large implications. Second, emergencies and special events should be taken into account in the timetabling problem as they may cause dramatic changes in the supply and demand of the URT services. Third, last train delay problem may cause less reachability, a valid rescheduling model or supplement service by other modes should be proposed. Fourth, the multimodal coordination of the last trains has large implications for passenger travel arrangements and thus should be well-tuned in recommendation systems of multimodal trip and activity scheduling (Zhang et al., 2011; Liao et al., 2013). Finally, the coordination with 24-h service buses would effectively improve the passenger accessibility in the late evening.

#### CRediT authorship contribution statement

**Kang Huang:** Conceptualization, Methodology, Validation, Writing - original draft. **Jianjun Wu:** Conceptualization, Methodology, Writing - review & editing, Supervision. **Feixiong Liao:** Conceptualization, Methodology, Writing - review & editing, Supervision. **Huijun Sun:** Methodology, Writing - review & editing. **Fang He:** Methodology, Writing - review & editing. **Ziyu Gao:** Resources, Methodology, Writing - review & editing.

#### Acknowledgements

This work is supported by the National Key R&D Program of China (2019YFB1600200), National Natural Science Foundation of China (71771018, 71890972/71890970, 71621001), the China National Funds for Distinguished Young Scientists (71525002), the State Key Laboratory of Rail Traffic Control and Safety (No. RCS2020ZZ001).

#### Appendix A

##### Tables A1–A4

**Table A1**

Station IDs.

1	Gongzhufen	21	National Library	41	Zhuxinzhuang
2	Military Museum	22	Pinganli	42	Huoying
3	Fuxinmen	23	Caishikou	43	Olympic Green
4	Xidan	24	Beijing South Railway Station	44	Beitucheng
5	Dongdan	25	Jiaomenxi	45	Yongdingmenwai
6	Jianguomen	26	Lishuiqiao	46	Liuqiao
7	Guomao	27	Datunludong	47	Qilizhuang
8	Dawanglu	28	Huixinxijienanlou	48	Guoongzhuang
9	Xizhimen	29	Dongsi	49	Bagou
10	Gulou dajie	30	Ciqikou	50	Zhichunlu
11	Yonghe gong	31	Puhuangyu	51	Shaoyaoju
12	Dongzhimen	32	Songjia zhuang	52	Sanyuanqiao
13	Chaoyangmen	33	Cishousi	53	Shilihe
14	Beijing Railway Station	34	Baishiqiao S	54	Xiju
15	Chaowenmen	35	Nanluo guxiang	55	Xierqi
16	Hepingmen	36	Hujialou	56	Wangjingxi
17	Xuanwumen	37	Jintailu	57	Wangjing
18	Chegongzhuang	38	Beijing West Railway Station	58	Airport Terminal 3
19	Xiyuan	39	Zhushikou	59	Airport Terminal 2
20	Haidianhuangzhaung	40	Jiulongshan		

**Table A2**

Line and station properties.

	Stations										
Line1	1	2	3	4	5	6	7	8			
Line2	10	11	12	13	14	6	15	17	3	18	9
Line4	19	20	21	9	22	4	17	23	24	25	
Line5	26	27	28	11	29	5	15	30	31	32	
Line6	33	34	18	22	35	29	13	36	37		
Line7	38	23	39	30	40						
Line8N	41	42	43	44	10	35					
Line8S	39	45									
Line9	21	34	2	38	46	47					
Line10	20	50	44	28	51	52	36	7	53	32	25
Line13	9	50	55	42	26	56	51	12		54	46
Line14W	47	54								1	33
Line14E	57	37	8	40	53	31	45	24			
Line15	43	27	56	57							
Line16	19										
LineCP	55	41									
LineYZ	32										
LineAL	12	52	58	59							

LineAL: Airport Express.

**Table A3**Travel time from starting station to  $s$  station in the direction  $m$  on the  $l$  line ( $r_{ls}^m$ ).

Up-direction	Travel time (min)										
	Line1	20	23	30	32	41	43	48	51		
Line2	3	7	11	15	20	18	23	29	34	39	43
Line4	4	13	19	25	28	35	37	38	43	48	
Line5	6	15	20	26	32	36	38	40	45	49	
Line6	18	23	28	30	35	39	41	46	49		
Line7	0	9	14	17	26						
Line8N	0	12	30	35	42	47					
Line8S	0	5									
Line9	0	2	8	11	17	21					
Line10	5	6	17	22	25	29	38	42	50	58	66
Line13	0	7	19	29	35	45	48	55		82	85
Line14W	15	16								91	96
Line14E	6	24	27	30	38	44	48	51			
Line15	7	12	18	21							
Line16	0										
LineCP	0	9									
LineYZ	0										
LineAL	0	4	22	40							
Down-direction	Travel time (min)										
	Line1	35	34	27	24	16	14	9	6		
Line2	38	34	30	26	21	23	18	11	7	2	0
Line4	77	69	61	57	52	47	45	42	37	33	
Line5	43	34	30	23	17	13	11	9	4	0	
Line6	67	62	57	55	50	47	44	39	36		
Line7	43	34	30	26	17						
Line8N	49	37	20	14	7	2					
Line8S	30	35									
Line9	31	29	24	21	14	11					
Line10	94	92	81	77	74	69	61	57	48	40	32
Line13	57	50	35	26	21	10	7	0		15	13
Line14W	1	0								7	2
Line14E	45	27	24	21	13	8	3	0			
Line15	52	47	41	38							
Line16	30										
LineCP	38	30									
LineYZ	34										
LineAL	40	36	0	18							

**Table A4**

The original departure time from the starting station of the last train in different lines.

Lines	Up-direction	Down-direction
Line1	23:30	23:30
Line2	23:03	23:00
Line4	22:20	22:38
Line5	22:48	23:11
Line6	22:25	22:49
Line7	23:15	22:25
Line8N	22:05	23:05
Line8S	23:35	23:30
Line9	23:19	22:40
Line10	22:31	22:42
Line13	22:42	22:42
Line14W	22:10	22:10
Line14E	22:30	22:40
Line15	23:15	22:11
Line16	22:55	22:50
LineCP	23:35	22:50
LineYZ	23:20	22:40
LineAL	22:30	23:10

## References

- An, K., Lo, H.K., 2016. Two-phase stochastic program for transit network design under demand uncertainty. *Transp. Res. Part B* 84, 157–181.
- Binder, S., Maknoon, Y., Bierlaire, M., 2017. The multi-objective railway timetable rescheduling problem. *Transp. Res. Part C* 78, 78–94.
- Canca, D., De-Los-Santos, A., Laporte, G., Mesa, J.A., 2017. An adaptive neighborhood search metaheuristic for the integrated railway rapid transit network design and line planning problem. *Comput. Oper. Res.* 78, 1–14.
- Canca, D., Zarzo, A., 2017. Design of energy-efficient timetables in two-way railway rapid transit lines. *Transp. Res. Part B* 102, 142–161.
- Canca, D., Barrena, E., 2018. The integrated rolling stock circulation and depot location problem in railway rapid transit systems. *Transp. Res. Part E* 109, 115–138.
- Canca, D., De-Los-Santos, A., Laporte, G., Mesa, J.A., 2019. Integrated Railway Rapid Transit Network Design and Line Planning problem with maximum profit. *Transp. Res. Part E* 127, 1–30.
- Chen, Y., Mao, B., Bai, Y., Ho, T.K., Li, Z., 2019a. Timetable synchronization of last trains for urban rail networks with maximum accessibility. *Transp. Res. Part C* 99, 110–129.
- Chen, Y., Mao, B., Bai, Y., Ho, T.K., Li, Z., 2019b. Optimal coordination of last trains for maximum transfer accessibility with heterogeneous walking time. *J. Adv. Transp.* 2019, 969204.
- Dou, X., Meng, Q., Guo, X., 2015. Bus schedule coordination for the last train service in an intermodal bus-and-train transport network. *Transp. Res. Part C* 60, 360–376.
- Dou, X., Guo, X., 2017. Schedule Coordination Method for Last Train Transfer Problem. *Transp. Res. Board* 2648 (1), 86–95.
- Fu, H., Nie, L., Meng, L., Sperry, B.R., He, Z., 2015. A hierarchical line planning approach for a large-scale high-speed rail network: the China case. *Transp. Res. Part A* 75, 61–83.
- Gao, Y., Kroon, L., Schmidt, M., Yang, L., 2016. Rescheduling a metro line in an over-crowded situation after disruptions. *Transp. Res. Part B* 93, 425–449.
- Goossens, J.W., van Hoesel, S., Kroon, L., 2006. On solving multi-type railway line planning problems. *Eur. J. Oper. Res.* 168 (2), 403–424.
- Guo, X., Wu, J., Zhou, J., Yang, X., Wu, D., Gao, Z., 2018. First-train timing synchronisation using multi-objective optimisation in urban transit networks. *Int. J. Prod. Res.* 57 (11), 3522–3537.
- Guo, X., Sun, H., Wu, J., Jin, J., Zhou, J., Gao, Z., 2016. Multiperiod-based timetable optimization for metro transit networks. *Transp. Res. Part B* 96, 46–67.
- Guo, X., Wu, J., Sun, H., Yang, X., Jin, J., Wang, Z., 2020. Scheduling synchronization in urban rail transit networks: Trade-offs between transfer passenger and last train operation. *Transp. Res. Part A* 138, 463–490.
- Gunantara, N., 2018. A review of multi-objective optimization: Methods and its applications. *Cogent Eng.* 5 (1), 1502242.
- Gutiérrez-Jarpa, G., Laporte, G., Marianov, V., 2018. Corridor-based metro network design with travel flow capture. *Comput. Oper. Res.* 89, 58–67.
- Hassannayebi, E., Zegordi, S.H., Yaghini, M., 2016. Train timetabling for an urban rail transit line using a Lagrangian relaxation approach. *Appl. Math. Model.* 40 (23–24), 9892–9913.
- Hassannayebi, E., Zegordi, S.H., 2017. Variable and adaptive neighbourhood search algorithms for rail rapid transit timetabling problem. *Comput. Oper. Res.* 78, 439–453.
- Hassannayebi, E., Boroun, M., Jordehi, S.A., Kor, H., 2019. Train schedule optimization in a high-speed railway system using a hybrid simulation and meta-model approach. *Comput. Ind. Eng.* 138, 106110.
- Huang, K., Wu, J., Yang, X., Gao, Z., Liu, F., Zhu, Y., 2019. Discrete Train Speed Profile Optimization for Urban Rail Transit: A Data-Driven Model and Integrated Algorithms Based on Machine Learning. *J. Adv. Transp.* 2019, 7258986.
- Jin, J.G., Zhao, J., Lee, D.H., 2013. A column generation based approach for the train network design optimization problem. *Transp. Res. Part E* 50, 1–17.
- Kang, L., Wu, J., Sun, H., Zhu, X., Gao, Z., 2015a. A case study on the coordination of last trains for the Beijing subway network. *Transp. Res. Part B* 72, 112–127.
- Kang, L., Wu, J., Sun, H., Zhu, X., Wang, B., 2015b. A practical model for last train rescheduling with train delay in urban railway transit networks. *Omega* 50, 29–42.
- Kang, L., Meng, Q., 2017. Two-phase decomposition method for the last train departure time choice in subway networks. *Transp. Res. Part B* 104, 568–582.
- Kang, L., Zhu, X., 2017. Strategic timetable scheduling for last trains in urban railway transit networks. *Appl. Math. Model.* 45, 209–225.
- Kang, L., Zhu, X., Sun, H., Wu, J., Gao, Z., Hu, B., 2019. Last train timetabling optimization and bus bridging service management in urban railway transit networks. *Omega* 84, 31–44.
- Liao, F., Arentze, T., Timmermans, H., 2013. Incorporating space-time constraints and activity-travel time profiles in a multi-state supernetwork approach to individual activity-travel scheduling. *Transp. Res. Part B* 55, 41–58.
- Lv, H., Zhang, Y., Huang, K., Yu, X., Wu, J., 2019. An Energy-Efficient Timetable Optimization Approach in a Bi-Direction Urban Rail Transit Line: A Mixed-Integer Linear Programming Model. *Energies* 12 (14), 2686.
- Niu, H., Zhou, X., 2013. Optimizing urban rail timetable under time-dependent demand and oversaturated conditions. *Transp. Res. Part C* 36, 212–230.
- Niu, H., Zhou, X., Gao, R., 2015. Train scheduling for minimizing passenger waiting time with time-dependent demand and skip-stop patterns: Nonlinear integer programming models with linear constraints. *Transp. Res. Part B* 76, 117–135.
- Ortega, F.A., Pozo, M.A., Puerto, J., 2018. On-Line Timetable Rescheduling in a Transit Line. *Transp. Sci.* 52 (5), 1106–1121.
- Shang, P., Li, R., Liu, Z., Yang, L., Wang, Y., 2018. Equity-oriented skip-stopping schedule optimization in an oversaturated urban rail transit network. *Transp. Res. Part C* 89, 321–343.

- Shang, P., Li, R., Guo, J., Xian, K., Zhou, X., 2019. Integrating Lagrangian and Eulerian observations for passenger flow state estimation in an urban rail transit network: A space-time-state hyper network-based assignment approach. *Transp. Res. Part B* 121, 135–167.
- Sun, H., Wu, J., Ma, H., Yang, X., Gao, Z., 2018. A bi-objective timetable optimization model for urban rail transit based on the time-dependent passenger volume. *IEEE Trans. Intell. Transp. Syst.* 20 (2), 604–615.
- Wong, R.C., Yuen, T.W., Fung, K.W., Leung, J.M., 2008. Optimizing timetable synchronization for rail mass transit. *Transp. Sci.* 42 (1), 57–69.
- Wu, J., Liu, M., Sun, H., Li, T., Gao, Z., Wang, D.Z., 2015. Equity-based timetable synchronization optimization in urban subway network. *Transp. Res. Part C* 51, 1–18.
- Xu, W., Zhao, P., Ning, L., 2018. A Practical Method for Timetable Rescheduling in Subway Networks during the End-of-Service Period. *J. Adv. Transp.* 2018, 5914276.
- Yang, S., Yang, K., Gao, Z., Yang, L., Shi, J., 2017. Last-train timetabling under transfer demand uncertainty: Mean-variance model and heuristic solution. *J. Adv. Transp.* 2017, 5095021.
- Yang, S., Wu, J., Yang, X., Liao, F., Li, D., Wei, Y., 2019a. Analysis of energy consumption reduction in metro systems using rolling stop-skipping patterns. *Comput. Ind. Eng.* 127, 129–142.
- Yan, F., Goverde, R.M., 2019. Combined line planning and train timetabling for strongly heterogeneous railway lines with direct connections. *Transp. Res. Part B* 127, 20–46.
- Yang, S., Liao, F., Wu, J., Timmermans, H., Sun, H., Gao, Z., 2020. A bi-objective timetable optimization model incorporating energy allocation and passenger assignment in an energy-regenerative metro system. *Transp. Res. Part B* 133, 85–113.
- Yang, X., Wu, J., Sun, H., Gao, Z., Yin, H., Qu, Y., 2019b. Performance improvement of energy consumption, passenger time and robustness in metro systems: A multi-objective timetable optimization approach. *Comput. Ind. Eng.* 137, 106076.
- Yao, Y., Zhu, X., Shi, H., Shang, P., 2019. Last train timetable optimization considering detour routing strategy in an urban rail transit network. *Meas. Control* 52 (9–10), 1461–1479.
- Yin, H., Wu, J., Sun, H., Kang, L., Liu, R., 2019. Optimizing last trains timetable in the urban rail network: social welfare and synchronization. *Transp. B: Transp. Dynam.* 7 (1), 473–497.
- Yue, Y., Han, J., Wang, S., Liu, X., 2017. Integrated train timetabling and rolling stock scheduling model based on time-dependent demand for urban rail transit. *Comput.-Aided Civ. Inf.* 32 (10), 856–873.
- Zhang, H., Jia, L., Wang, L., Xu, X., 2019. Energy consumption optimization of train operation for railway systems: Algorithm development and real-world case study. *J. Clean. Prod.* 214, 1024–1037.
- Zhang, J., Liao, F., Arentze, T., Timmermans, H., 2011. A multimodal transport network model for advanced traveler information systems. *Procedia Comput. Sci.* 5, 912–919.
- Zhou, Y., Wang, Y., Yang, H., Yan, X., 2019. Last train scheduling for maximizing passenger destination reachability in urban rail transit networks. *Transp. Res. Part B* 129, 79–95.
- Zhou, F., Shi, J., Pan, H., 2013. Optimization method for last train coordination plan of urban rail transit based on network operation. *Procedia-Soc. Behav. Sci.* 96, 2706–2712.
- Zhu, Y., Goverde, R.M., 2019. Railway timetable rescheduling with flexible stopping and flexible short-turning during disruptions. *Transp. Res. Part B* 123, 149–181.